



**HAL**  
open science

# Planar cell polarity regulators in asymmetric organogenesis during development and disease

De-Li Shi

► **To cite this version:**

De-Li Shi. Planar cell polarity regulators in asymmetric organogenesis during development and disease. JOURNAL OF GENETICS AND GENOMICS, 2022, 10.1016/j.jgg.2022.06.007 . hal-03719572

**HAL Id: hal-03719572**

**<https://hal.sorbonne-universite.fr/hal-03719572>**

Submitted on 11 Jul 2022

**HAL** is a multi-disciplinary open access archive for the deposit and dissemination of scientific research documents, whether they are published or not. The documents may come from teaching and research institutions in France or abroad, or from public or private research centers.

L'archive ouverte pluridisciplinaire **HAL**, est destinée au dépôt et à la diffusion de documents scientifiques de niveau recherche, publiés ou non, émanant des établissements d'enseignement et de recherche français ou étrangers, des laboratoires publics ou privés.

1 **Planar cell polarity regulators in asymmetric organogenesis during development**  
2 **and disease**

3 De-Li Shi<sup>a,b,\*</sup>

4 <sup>a</sup>Affiliated Hospital of Guangdong Medical University, Zhanjiang 524001, China

5 <sup>b</sup>Laboratory of Developmental Biology, CNRS-UMR7622, Institut de Biologie Paris-Seine (IBPS),  
6 Sorbonne University, 75005 Paris, France

7

8 \*Correspondence: de-li.shi@upmc.fr

9

10 Running title: Asymmetry in organ morphogenesis

11

11 **Abstract**

12           The phenomenon of planar cell polarity is critically required for a myriad of morphogenetic  
13 processes in metazoan and is accurately controlled by several conserved modules. Six “core”  
14 proteins, including Frizzled, Flamingo (Celsr), Van Gogh (Vangl), Dishevelled, Prickle, and Diego  
15 (Ankrd6), are major components of the Wnt/planar cell polarity pathway. The Fat/Dchs  
16 protocadherins and the Scrib polarity complex also function to instruct cellular polarization. In  
17 vertebrates, all these pathways are essential for tissue and organ morphogenesis, such as neural  
18 tube closure, left-right symmetry breaking, heart and gut morphogenesis, lung and kidney  
19 branching, stereociliary bundle orientation, and proximal-distal limb elongation. Mutations in  
20 planar polarity genes are closely linked to various congenital diseases. Striking advances have  
21 been made in deciphering their contribution to the establishment of spatially oriented pattern in  
22 developing organs and the maintenance of tissue homeostasis. The challenge remains to clarify  
23 the complex interplay of different polarity pathways in organogenesis and the link of cell polarity  
24 to cell fate specification. Interdisciplinary approaches are also important to understand the roles  
25 of mechanical forces in coupling cellular polarization and differentiation. This review outlines  
26 current advances on planar polarity regulators in asymmetric organ formation, with the aim to  
27 identify questions that deserve further investigation.

28 Key words: planar cell polarity, Wnt/PCP signaling, left-right asymmetry, heart and gut  
29 morphogenesis, lung and kidney branching, inner ear hair cell orientation, limb outgrowth

30

## 30 Introduction

31 Planar cell polarity (PCP), initially studied in the retina and the wing of insects *Oncopeltus*  
32 *fasciatus* and *Drosophila melanogaster* (Lawrence and Shelton, 1975; Gubb and García-Bellido,  
33 1982), refers to coordinated cellular orientation within the plane of an epithelium or a tissue. This  
34 fascinating process exerts wide functions in organizing the asymmetric cellular choreography and  
35 the spatially oriented pattern during tissue and organ morphogenesis, contributing to, for  
36 example, the architectural beauty of the *Drosophila* compound eye and the mammalian cochlea.  
37 The phenomenon of PCP is mostly regulated by a set of evolutionarily conserved proteins,  
38 including Frizzled receptors, Flamingo (Celsr1-3 in vertebrates), Dishevelled (Dvl1-3 in  
39 vertebrates), Diego (Ankrd6 in vertebrates), Van Gogh (Vangl1-2 in vertebrates), and Prickle  
40 (Prickle1-3 in vertebrates). These “core” PCP proteins transduce Wnt/PCP signaling to regulate  
41 cytoskeletal rearrangements and polarized cell behaviors in a variety of morphogenetic  
42 processes (Wallingford, 2012; Yang and Mlodzik, 2015; Henderson et al., 2018). Increasing  
43 evidence suggests that several vertebrate Wnts, such as Wnt5a and Wnt11, are also important  
44 components of the Wnt/PCP pathway, although they are not considered as “core” PCP proteins.

45 There are also other conserved protein complexes that function as important PCP  
46 regulators in *Drosophila* and vertebrates. The heteromeric protocadherins Fat4 and Dchs1  
47 (dachshous cadherin-related 1) represent the second PCP pathway (Fat/Dchs module) that is  
48 regulated by the Golgi resident transmembrane kinase Four-jointed or Fj (Blair and McNeill,  
49 2018). The Scrib (Scrb1 or Scribble1) polarity complex, originally identified as a regulator of  
50 apico-basal cell polarity, consists of Scrib, Dlg (Discs-large) and Lgl (Lethal-giant larvae) proteins  
51 (Milgrom-Hoffman and Humbert, 2018). These pathways exert broad activity in cellular signaling  
52 and cytoskeletal organization. They function in concert with or independently of the “core”  
53 Wnt/PCP pathway to regulate cell polarity. Two additional systems, the Fat2/Lar (leukocyte  
54 antigen-related receptor tyrosine phosphatase) and Toll-8/Cirl (adhesion G protein-coupled  
55 receptor) pathways, have been recently shown to instruct some *Drosophila* PCP processes, but  
56 their functions in vertebrates merit future investigation (Lavalou and Lecuit, 2022).

57           The “core” PCP pathway, the Fat/Dchs polarity module and the Scrib complex are  
58 critically involved in tissue and organ morphogenesis, from the emergence of organ primordia to  
59 terminal organogenesis and tissue homeostasis. In vertebrates, the functions of PCP proteins  
60 (herein collectively referred to as regulators of PCP-dependent cell behaviors) have been well  
61 documented in many morphogenetic processes, such as neural tube closure, embryonic left-right  
62 symmetry breaking, heart and gut morphogenesis, lung and kidney branching, orientation of inner  
63 ear hair cells, and proximal-distal limb bud elongation (Yang and Mlodzik, 2015; Henderson et al.,  
64 2018). Mutations of PCP genes impair organ development and are closely linked to various  
65 congenital anomalies, including neural tube defects (Wang et al., 2019), laterality disorders  
66 (Grimes and Burdine, 2017), hearing deficits (May-Simera and Kelley, 2012), lung and kidney  
67 diseases (Vladar and Königshoff, 2020; Torban and Sokol, 2021), as well as limb abnormalities  
68 (Gao and Yang, 2013). Importantly, PCP proteins regulate common cellular processes underlying  
69 the outgrowth and elongation of tissue primordia, such as convergent extension (CE) movements  
70 driven by oriented cell division and intercalation (Wallingford, 2012). Therefore, their dysfunctions  
71 can lead to multiple phenotypes, highlighting a general importance in organogenesis. There are  
72 many excellent reviews focusing on PCP functions in specific aspects of morphogenesis, but a  
73 more comprehensive analysis of PCP regulators during development of different organs that  
74 display PCP-dependent cellular organization is beneficial for understanding their complex  
75 interplay in the establishment of cell polarity. This review attempts to present past achievements  
76 and latest advances of PCP protein functions in asymmetric organogenesis, with the aim to  
77 identify challenges in deciphering the extraordinary process of asymmetry formation.

## 78 **Wnt signaling pathways and planar cell polarity protein complexes**

79           Vertebrate Wnt pathways can be divided into three branches based on the activation of  
80 different biological readouts (Fig. 1A). Wnt/ $\beta$ -catenin or canonical Wnt signaling induces target  
81 gene transcription and cell fate specification by stabilizing  $\beta$ -catenin through inhibition of its  
82 destruction complex. Non-canonical Wnt signaling includes Wnt/PCP and Wnt/ $\text{Ca}^{2+}$  branches that  
83 function independently of  $\beta$ -catenin. Wnt/PCP signaling controls cell polarity by regulating  
84 cytoskeletal rearrangements and/or transcriptional responses. It functions through several well-

85 characterized planar polarity effector (PPE) proteins, such as Daam1 (Dishevelled-associated  
86 activator of morphogenesis 1), Rho family of small GTPases and Jun N-terminal kinase (JNK),  
87 but also via a few less well-studied ciliogenesis and planar polarity effector (CPLANE) proteins  
88 including Intu, Fuz and Wdpcp (Adler and Wallingford, 2017). Wnt/Ca<sup>2+</sup> signaling triggers  
89 intracellular calcium flux to induce actin polymerization and NFAT (nuclear factor of activated T-  
90 cells)-mediated target gene transcription. Dvl family proteins function in all Wnt pathway branches  
91 through distinct domains including DIX, PDZ and DEP (Shi, 2020). Their conserved C-terminus  
92 PDZ domain-binding motif can modulate Wnt/ $\beta$ -catenin and Wnt/PCP signaling through  
93 interaction with the PDZ domain (Lee et al., 2015).

94 The “core” PCP proteins form two separate complexes that are distributed on opposite  
95 cell borders within the tissue plane (Fig. 1B,C). Frizzled (Fzd), Dvl and Ankrd6 reside on one side  
96 of the cell, while Vangl and Prickle localize to the opposite side. Celsr is present on both sides  
97 and forms homodimers between adjacent cells to propagate polarity information across cells.  
98 This asymmetric distribution of “core” PCP proteins is a hallmark of planar polarization and  
99 reflects the coordinated cellular orientation during tissue or organ morphogenesis. Vertebrate  
100 Wnt5a signaling gradient can provide global cues to instruct the asymmetric localization of “core”  
101 PCP proteins in several well-documented PCP-dependent processes, such as the proximal-distal  
102 development of limb bud and the anteroposterior (AP) polarization of node cells (Gao et al., 2011;  
103 Minegishi et al., 2017). Similarly, Fat and Dchs heteromeric protocadherins are localized to  
104 opposite sides of adjacent cells (Fig. 1B), and they may function either as a ligand or as a  
105 receptor for the other to mediate cell interaction (Blair and McNeill, 2018). Through a multitude of  
106 biochemical, functional and genetic interactions, PCP proteins regulate non-canonical Wnt  
107 signaling and make an important contribution to the spatiotemporal organization of cellular  
108 activities in a variety of tissues and organs (Table 1). The following sections will detail their  
109 implications in asymmetric organ morphogenesis during development and disease.

### 110 **Early embryonic left-right asymmetry**

111 Left-right asymmetry, either external or internal, is a common feature in animals. Although  
112 vertebrate embryos are seemingly symmetrical, they already display asymmetric gene expression

113 at early stages of development. This is critical for the asymmetric formation of internal organ  
114 primordia and their subsequent morphogenesis to generate left-right differences in sizes, shapes  
115 and anatomical locations. Transient structures formed during early development, such as the  
116 posterior gastrocoel roof plate (GRP) in *Xenopus*, the Kupffer's vesicle (KV) in zebrafish, the  
117 Hensen's node in chick and the node in mice, constitute the left-right organizer (LRO) involved in  
118 breaking the bilateral symmetry across the mediolateral plane (Fig. 2A,B). They initiate left-right  
119 asymmetry by providing instructive signals mostly through cilia-mediated directional fluid flow  
120 (Axelrod, 2020; Little and Norris, 2021). Wnt/PCP signaling acts in the LRO to coordinate the  
121 orientation of individual cells and multicellular structures with respect to the embryonic axes.  
122 Subsequently, signals generated in a manner that is both dependent and independent on motile  
123 cilia create a gradient of Nodal protein to activate left-sided expression of the Nodal-Lefty-Pitx2  
124 network (Grimes and Burdine, 2017; Axelrod, 2020). Thus, differential gene activation and  
125 repression establish left-right embryonic polarity that will influence the asymmetric  
126 morphogenesis of organ primordia.

127 Dvl, Vangl and Prickle are important for cilia-dependent asymmetric fluid flow. In node  
128 cells, Vangl1, Vangl2 and Prickle2 are localized to the anterior side, while Dvl2 and Dvl3 are  
129 enriched at the posterior side (Antic et al. 2010; Hashimoto et al., 2010; Grimes and Burdine,  
130 2017). Wnt5a and Wnt5b, which are expressed posteriorly relative to the node, form a diffusible  
131 gradient and provide instructive signals to induce the asymmetric localization of Vangl1 and  
132 Prickle2, thus polarizing node cells along the AP axis (Minegishi et al., 2017). The asymmetric  
133 localization of "core" PCP proteins then restricts the posterior positioning of ciliary basal bodies at  
134 the dome-shaped apical surfaces of node cells and promotes the posterior tilting of cilia by  
135 coordinating the asymmetric distribution of microtubules and actomyosin networks (Sai et al.,  
136 2022). Subsequently, cilia-driven leftward fluid flow across the node initiates left-right asymmetry.  
137 Knockout of Dvl2 and Dvl3 impairs the posterior location of ciliary basal bodies (Hashimoto et al.,  
138 2010). Loss of Vangl1 and Vang2 disrupts the posterior orientation of primary motile cilia in the  
139 LRO, resulting in defective expression of Nodal and Pitx2 on the left side (Borovina et al., 2010;  
140 Antic et al., 2010; Song et al., 2010). Consistent with their association into a complex, Prickle1

141 and Prickle2 interact with Vangl2 to regulate its anterior localization in node cells (Minegishi et al.,  
142 2017), while Prickle3 shows reciprocal interactions with Vangl2 for the anterior localization in  
143 GRP cells to promote growth and posterior positioning of motile cilia (Chu et al., 2016).  
144 Downstream of “core” PCP proteins, JNK activity is required for modulating ciliogenesis and cilia  
145 length in the zebrafish KV (Derrick et al., 2022). Altogether, these observations reveal an  
146 important implication of Wnt/PCP signaling in the orientation of motile cilia within the LRO. Thus,  
147 the AP polarity generated by the asymmetric distribution of PCP proteins can be translated into  
148 left-right asymmetry through the directional fluid flow.

149         The unconventional Myosin1D (Myo1D) also functions to shape the cilia-driven directional  
150 fluid flow in the LRO, although unlikely being a component of the Wnt/PCP pathway. It interacts  
151 with Vangl2 to initiate left-right axis formation in zebrafish and *Xenopus* embryos (Juan et al.,  
152 2018; Tingler et al., 2018). In the zebrafish KV, Myo1D antagonizes the activity of Vangl2 to  
153 restrict the localization of posteriorly pointing cilia at the anterior region and anteriorly pointing  
154 cilia at the posterior region, thereby establishing a circular geometry of fluid flow (Juan et al.,  
155 2018). Thus, the cilia-dependent function of Myo1D acts in concert with Wnt/PCP signaling to  
156 break left-right symmetry.

### 157 **Asymmetric cardiac morphogenesis**

158         The rightward looping of the heart primordium contributes to determine the relative  
159 position of cardiac chambers and is the first event of asymmetric organogenesis (Desgrange et  
160 al., 2018). It is initiated by the transformation of the cardiac tube into a loop (Fig. 2C). Abnormal  
161 left-right patterning is intimately associated with congenital heart diseases, such as X-linked  
162 heterotaxy caused by mutations of the ZIC3 transcription factor. Recent evidence suggests that  
163 Zic3 regulates the expression of PCP genes and is required for Dvl phosphorylation during node  
164 morphogenesis. It also genetically interacts with PCP genes to establish the left-right heart  
165 asymmetry (Bellchambers and Ware, 2021). Therefore, there is a possibility that dysregulation of  
166 PCP proteins may represent an underlying mechanism of ZIC3 mutations in congenital disorders  
167 associated with heterotaxy.



168 Wnt/PCP signaling critically regulates heart morphogenesis after looping, particularly  
169 directional cell movements from the second heart field (SHF) during outflow tract (OFT)  
170 development (Henderson et al., 2006). Wnt5a, Wnt5b and Wnt11 are important for modulating  
171 extracellular matrix composition, cytoskeletal rearrangements, actomyosin contractility, and cell  
172 adhesion during SHF deployment and heart tube remodeling (Zhou et al., 2007; Sinha et al.,  
173 2015; Merks et al., 2018). Loss of Wnt5a in mice leads to OFT malformations due to impaired cell  
174 deployment in the SHF (Sinha et al., 2015). Moreover, Wnt5a functions through Daam1 in OFT  
175 morphogenesis by promoting the AP elongation of the SHF (Li et al., 2019).

176 Dvl family members collectively contribute to OFT morphogenesis. Loss of Dvl1 and Dvl2  
177 impairs SHF deployment and OFT lengthening by disrupting actin polymerization and filopodia  
178 formation (Sinha et al., 2012). Homozygous *Looptail* mice, which carry a single nucleotide  
179 mutation in the *Vangl2* gene that is predicted to produce a malfunctional Vangl2 protein, show  
180 defects in the polarization of myocardial cells likely due to reduced activity of RhoA and ROCK1  
181 (Rho-associated kinase 1). As a consequence, myocardializing cells fail to extend cellular  
182 protrusions into the OFT cushion, resulting in abnormal muscularization of the proximal outlet  
183 septum (Phillips et al., 2005). Conditional knockout of Vangl2 indicates that it is solely required  
184 within the SHF to promote lengthening of the OFT by regulating cellular polarity in the distal  
185 outflow wall (Ramsbottom et al., 2014). Similarly, loss of Prickle1 in mice leads to shortened OFT  
186 due to absence of polarized cell orientation in the SHF (Gibbs et al., 2016). Conditional knockout  
187 of Daam1 in the myocardium prevents cardiomyocytes from extending protrusions into the OFT  
188 (Ajima et al., 2015). Disruption of the CPLANE protein Wdpcp in mice also prevents polarized  
189 migration of cardiomyocytes to invade the OFT cushion and causes OFT septation defects (Cui  
190 et al., 2013). Thus, Wnt/PCP signaling coordinates directional cell migration in the SHF to  
191 promote heart morphogenesis.

192 PCP proteins are also involved in other aspects of heart development. In mice, Fzd4 is  
193 required for arterial and arteriolar formation. It cooperates with Dvl3 to regulate vascular cell  
194 proliferation and migration through microtubule stabilization and cellular polarization (Descamps  
195 et al., 2012). Fzd2 and Fzd7 are redundantly required for CE movements to promote closure of

196 the ventricular septum (Yu et al., 2012). Vangl2 interacts with RhoA and ROCK in the formation  
197 of the coronary vasculature through a non-autonomous manner, likely by regulating deposition of  
198 fibronectin in the subepicardial space for the migration of epicardially-derived cells (Phillips et al.,  
199 2008). Combined loss of Daam1 and Daam2 in mice causes severe cardiac abnormalities  
200 including ventricular noncompaction, ventricular septal defects, irregular sarcomere assembly,  
201 and impaired myocardial maturation (Li et al., 2011; Ajima et al., 2015). However, it is unclear  
202 whether these defects are all direct consequences of disrupted Wnt/PCP signaling.

### 203 **Gut looping and elongation**

204 The left-right asymmetry of the developing gut arises through an important morphogenetic  
205 process known as gut looping. This event has been shown to rely on physical forces generated  
206 by differential growth rates between the gut and the dorsal mesentery that connects the gut to the  
207 body wall (Savin et al., 2011). The earliest left-right asymmetric gut morphology is manifested by  
208 the leftward curvature of the stomach (Fig. 2D). In the chick embryo, Nodal-induced expression of  
209 Pitx2 maintains left-side identity of the early gut tube (Huycke and Tabin, 2018; Grzymkowski et  
210 al., 2020). Wnt/PCP signaling acts downstream of Pitx2 to coordinate asymmetric processes of  
211 the digestive system, including gut looping, intestine elongation, villification of the intestinal  
212 epithelium, stem cell lineage segregation, and maintenance of epithelial homeostasis.

213 Several PCP proteins display asymmetric expression in the chicken dorsal mesentery,  
214 which exhibits polarized cellular behaviors with extensive membrane contacts between adjacent  
215 mesenchymal cells on the left side. Fzd4 and Daam2 show Pitx2-dependent left-sided  
216 expression, and Daam2 is required for cell adhesion necessary for mesenchymal condensation in  
217 the dorsal mesentery (Welsh et al., 2013). Although Wnt5a does not display asymmetric  
218 expression, its activity on the right side is antagonized by the right-sided expression of secreted  
219 Frizzled-related proteins (sFRPs). Therefore, the asymmetric activation of Wnt5a-Fzd4-Daam2  
220 pathway triggers leftward tilt of the midgut (Welsh et al., 2013).

221 Intestine elongation critically requires functional PCP signaling. In mice, Wnt5a is  
222 expressed in the gut mesenchyme. Constitutive knockout of Wnt5a disrupts midgut elongation by  
223 preventing post-mitotic daughter cells from re-intercalating into the epithelial layer (Cervantes et

224 al., 2009) as well as from extending filopodia for basal return of their nuclei during interkinetic  
225 nuclear migration (Wang et al., 2018). Ror2 and Ryk differentially regulate midgut elongation  
226 through dynamic spatiotemporal interactions with Wnt5a. Mesenchyme-derived Ror2 functions  
227 before the early phase of midgut elongation, while both epithelial and mesenchymal Ryk  
228 contributes to midgut elongation throughout the early phase (Wang et al., 2020). Vangl2  
229 regulates several polarized cell behaviors in the gut epithelium to couple epithelial  
230 morphogenesis with gut tube elongation. In mice, it functions with Wnt5a for oriented cell division  
231 along the rostrocaudal axis to increase fore-stomach length (Matsuyama et al., 2009). In  
232 *Xenopus*, Vangl2 is enriched at the apical and anterior surfaces of radially elongated gut  
233 endoderm cells; it coordinates microtubule organization, cell adhesion and endodermal cell shape  
234 changes to promote gut elongation and lumen formation (Dush and Nascone-Yoder, 2019). At  
235 late stages of intestine elongation, the Fat4/Dchs1 module acts in parallel with Vangl2 to drive  
236 mesenchymal cell clustering necessary for epithelial folding during villus formation, while Wnt5a  
237 functions upstream of Fat4 and acts as a chemoattractant to guide directional migration of  
238 mesenchymal cells (Rao-Bhatia et al., 2020).

239 The gene encoding cilia and flagella associated protein 126, *Cfap126* (also known as  
240 *Flattop* or *Fltp*), is transcriptionally activated during Wnt/PCP acquisition in ciliated cells, thus  
241 representing a target of Wnt/PCP signaling (Gegg et al., 2014). *Cfap126* can function as a PPE,  
242 and its transient expression in *Lgr5*<sup>+</sup> intestinal stem cells regulates lineage priming and cell cycle  
243 exit at the base of the crypt, contributing to the differentiation of Paneth and enteroendocrine cells  
244 (Böttcher et al., 2021). In the adult, Wnt5a is expressed in *FoxL1*<sup>+</sup> telocytes at the crypt-villus  
245 junction regions and is required for homeostatic renewal of the intestinal epithelium (Shoshkes-  
246 Carmel et al., 2018). These data highlight an essential role of Wnt/PCP signaling in intestinal  
247 stem cell lineage segregation and directly link cell polarity to cell fate specification.

## 248 **Lung branching morphogenesis**

249 The highly elaborated and polarized architecture of the respiratory system emerges from  
250 reciprocal interactions between lung epithelium and mesenchyme (Fig. 3A). Lung branching  
251 morphogenesis involves repetitive formation of new buds, epithelial sprouting, and tube

252 elongation to generate an arborized airway network. This process is also dependent on several  
253 aforementioned asymmetric cell behaviors. PCP proteins regulate different aspects of lung  
254 morphogenesis, and their dysfunctions are linked to lung diseases, such as emphysema, a  
255 chronic obstructive pulmonary disease, also known as COPD (Vladar and Königshoff, 2020).

256 In the mouse embryo, *Wnt5a* is mainly expressed in the mesenchyme of branch points  
257 and functions through *Ror2* to synchronize radial polarization of mesenchymal cells for tube  
258 elongation along the AP axis (Kishimoto et al., 2018). It also activates the *Ror2-Vangl2* cascade  
259 in both lung epithelium and mesenchyme to coordinate alveolar formation through cytoskeleton-  
260 mediated cell shape changes of alveolar type I cells and migration of myofibroblasts. Moreover,  
261 *Wnt5a* and *Vangl2* show reduced expression in lung tissues of human patients with  
262 bronchopulmonary dysplasia and emphysema, suggesting a possible implication of these genes  
263 in lung diseases (Li et al., 2020; Zhang et al., 2020). *Fzd2* regulates epithelial cell shape changes  
264 to promote branch point formation through RhoA-induced apical localization of phosphorylated  
265 myosin light chain 2 (Kadzic et al., 2014). *Celsr1* and *Vangl2* are enriched at the basal/luminal  
266 surface of branching lung epithelial buds. They regulate cytoskeletal remodeling likely via ROCK  
267 to maintain epithelial architecture, thus their mutations lead to a reduced number of epithelial  
268 branches (Yates et al., 2010b). Tracheal and alveolar epithelial cells from heterozygous *Looptail*  
269 mice show highly disrupted actomyosin networks and abnormal focal adhesions, which are  
270 correlated with decreased RhoA activity and reduced YAP signaling, suggesting that *Vangl2* may  
271 function as a regulator of mechanotransduction (Cheong et al., 2020). *Scrib* is required for lumen  
272 morphogenesis. It maintains tight junction integrity and epithelial cohesion through interaction  
273 with Wnt/PCP signaling by modulating the localization of *Celsr1* and *Vangl2* in lung epithelium  
274 (Yates et al., 2013).

275 Airway motile cilia present distinct orientations and highly coordinated movements, which  
276 are important for mucociliary clearance. During ciliogenesis, asymmetrically localized PCP  
277 complexes first polarize epithelial cells along the proximal (oral) to distal axis, and then provide  
278 polarity cues to orient ciliary basal bodies in the proximal direction (Vladar et al., 2016). In airway  
279 epithelia, *Fzd3*, *Fzd6*, *Dvl1* and *Dvl3* are enriched at the proximal side of multiciliated cells;

280 Vangl1, Vangl2 and Prickle2 are distributed at the distal side (Vladar et al., 2012, 2016); Dvl2 and  
281 Ankrd6 are localized to the base of cilia (Vladar et al., 2012). Loss of PCP protein expression or  
282 localization leads to mis-orientations of airway cilia and chronic inflammatory lung diseases  
283 (Vladar et al., 2012, 2016), suggesting an essential role of PCP signaling in maintaining lung  
284 homeostasis during fetal and post-natal development. Indeed, conditional knockout of Vangl1 or  
285 Prickle2 in mice impairs tracheal epithelial regeneration (Vladar et al., 2016); reducing the activity  
286 of Vangl2 causes tissue damage as observed in emphysema and impairs adult lung function  
287 (Poobalasingam et al., 2017). Knockout of Cfap126 mostly reduces the diameter of terminal lung  
288 bronchioles, leading to constricted distal airways in the post-natal lung (Gegg et al., 2014).

289 Wnt/PCP signaling also coordinates the development of pulmonary airway and  
290 vasculature. Wnt5a interacts with Ror2 to direct avian pulmonary vasculogenesis by regulating  
291 VEGF signaling through fibronectin expression in the mesenchyme (Loscertales et al., 2008).  
292 Pericytes are perivascular cells that promote vessel maturation. Loss of Wnt5a and Fzd7 impairs  
293 endothelium-pericyte interactions during pulmonary angiogenesis by disrupting the motility and  
294 polarity of pericytes, which may contribute to pulmonary arterial hypertension (Yuan et al., 2019).  
295 Since PCP proteins are critically involved in lung development, homeostasis and disease, it will  
296 be important to further decipher the mechanisms by which they orchestrate stage-specific cellular  
297 activities, ranging from epithelial-mesenchymal interactions in branching morphogenesis to the  
298 maturation of multiciliated cells and the development of respiratory vasculature.

### 299 **Kidney development**

300 The morphogenesis of the early urinary tract involves reciprocal interactions between the  
301 Wolffian duct-derived ureteric bud and its adjacent metanephric mesenchyme. Strikingly, the  
302 ureteric bud undergoes reiterative branching morphogenesis with distal elements engaged in  
303 directed cell migration, oriented cell division, and cell intercalation. These PCP-dependent cellular  
304 behaviors play important roles in ureteric bud branching, tubular elongation, and tubule diameter  
305 establishment (Carroll and Yu, 2012). Different polarity pathways are critically implicated in  
306 kidney development and potentially linked to various genetic disorders, such as congenital

307 malformations of the kidney and urinary tract (CAKUT) and glomerular diseases (Torban and  
308 Sokol, 2021).

309 It is well documented that Wnt ligands are essential in kidney morphogenesis. Pioneer  
310 studies have demonstrated a requirement of Wnt4 for mesenchymal to epithelial transformation  
311 that results in epithelialization of the ureteric bud (Stark et al., 1994; Kispert et al., 1998). Wnt5a-  
312 Ror2 signaling regulates epithelial tubular formation from the ureteric bud. Loss of Wnt5a or Ror2  
313 in mice impairs the positioning of metanephric mesenchyme and causes its aberrant interaction  
314 with the Wolffian duct, resulting in duplicated ureters and kidneys (Nishita et al., 2014; Yun et al.,  
315 2014). Wnt9b acts through Rho/JNK signaling to regulate CE movements and maintain polarized  
316 cell divisions in the epithelium during early stages of kidney morphogenesis, thus inhibition of  
317 Wnt9b-mediated signaling affects epithelial polarity and causes increased tubule diameter  
318 (Karner et al., 2009). Wnt11 derived from the ureteric branch tip promotes the stable attachment  
319 of nephron progenitors to the epithelial tip by regulating their polarity and motile behaviors,  
320 thereby maintaining nephrogenic niche integrity (O'Brien et al., 2018).

321 Several “core” PCP proteins clearly display asymmetric localization in developing renal  
322 tubule epithelia along the proximal-distal axis. In both the collecting duct and proximal tubules,  
323 Vangl1 and Vangl2 are accumulated at the proximal side, while Fzd3 and Fzd6 are distributed at  
324 the distal side, suggesting that they are involved in the polarization of renal tubules (Kunimoto et  
325 al., 2017). Functional analyses indicate that other “core” PCP proteins are also important for renal  
326 tubule morphogenesis. Mice deficient for Fzd4 and Fzd8 show renal hypoplasia, with delayed  
327 growth, branching and proliferation of the ureteric epithelium (Ye et al., 2011). However, these  
328 phenotypes may also result from disrupted Wnt/ $\beta$ -catenin signaling. Perturbation of Dvl function  
329 in *Xenopus* disrupts rosette-based CE movements driven by mediolaterally oriented cell  
330 intercalations, resulting in shorter and wider kidney tubules (Lienkamp et al., 2012). Vangl2  
331 regulates morphogenetic processes in the ureteric bud and metanephric mesenchyme.  
332 Homozygous *Looptail* mice show defective ureteric branching and glomerular maturation but with  
333 normal ureteric bud formation, consistent with impaired CE movements (Yates et al., 2010a).  
334 Prickle1 is required for tubule morphogenesis by regulating the distribution of actin cytoskeleton

335 in the ureteric bud; its loss of function impairs cell arrangements in the collecting duct and renal  
336 tubules, resulting in abnormal tubule shape (Liu et al., 2014). *Celsr1* genetically interacts with  
337 *Vangl2* to regulate rostrocaudal patterning of renal tubules and maturation of glomeruli; it also  
338 promotes ureteric tree growth during early stages of kidney development but prevents tubule  
339 overgrowth at late stages (Brzóška et al., 2016). Consistent with these functions, mutations of  
340 *CELSR1* are associated with renal disorders, including unilateral renal agenesis, hydronephrosis,  
341 and hydroureter (Brzóška et al., 2016). Therefore, it will be important to understand the molecular  
342 and cellular mechanisms underlying the stage-specific functions of *Celsr1* in kidney development.

343       Effectors of Wnt/PCP signaling are implicated in different aspects of renal tubule  
344 development. In *Xenopus* and zebrafish pronephros, *Daam1* may function through Rho GTPase  
345 to regulate cytoskeletal rearrangements for proper tubulogenesis and tubule morphology (Miller  
346 et al., 2011). It also colocalizes with E-cadherin at cell-cell contact regions in the *Xenopus* nephric  
347 primordium to ensure intercellular adhesion and epithelial tissue organization during CE  
348 movements (Krneta-Stankic et al., 2021). In mice, *Fuz* appears to regulate ureteric bud branching  
349 morphogenesis through cilia-dependent and -independent pathways, raising the possibility that it  
350 may play a role in ciliogenesis (Wang et al., 2021).

351       *Fat* and *Dchs* heteromeric protocadherins are important for cell interactions in the  
352 developing kidney. Loss of *Fat4* disrupts polarized cell behaviors and leads to cyst formation  
353 (Saburi et al., 2008). *Fat1* cooperates with *Fat4* in renal tubular elongation (Saburi et al., 2012).  
354 Importantly, the interaction between *Fat4* and *Dchs1* is necessary for ureteric bud branching and  
355 tubule diameter establishment. *Dchs1* is specifically expressed in the cap (condensing)  
356 mesenchyme that coalesces around the ureteric bud, while *Fat4* is only present in stromal cells  
357 that surround the cap mesenchyme (Fig. 3B). These expression patterns establish a crosstalk  
358 whereby *Fat4* interacts with *Dchs1* to regulate self-renewal and differentiation of ureteric epithelial  
359 progenitors through Hippo, Notch or FGF signaling (Das et al., 2013; Bagherie-Lachidan et al.,  
360 2015). *Fat4/Dchs1*-mediated stroma-to-cap signaling may also function to polarize the cap  
361 mesenchyme for proper nephrogenesis (Mao et al., 2015). There is also a complex interplay  
362 between *Fat* family protocadherins and other signaling pathways during kidney development. In

363 zebrafish pronephros, Fat1 functions with Scrib in Hippo signaling through regulation of YAP1.  
364 Depletion of Fat1 and Scrib causes severe cyst formation, suggesting that Scrib may couple Fat1  
365 with the Hippo pathway to coordinate cellular polarization and growth (Skouloudaki et al., 2009).  
366 In mice, Fat4 can act non-autonomously to prevent ectopic ureteric bud formation and kidney  
367 duplication by fine-tuning the signaling function of nephric duct-expressed RET, a GDNF receptor  
368 that regulates cell rearrangements in ureteric bud morphogenesis (Zhang et al., 2019). Thus,  
369 Fat4 plays a critical role in the cap mesenchyme to control the nephron progenitor pool.

370 Wnt/PCP signaling is also important for proper organization of podocytes, which are highly  
371 specialized and polarized glomerular visceral epithelial cells that are essential for maintaining the  
372 correct function of the glomerular filtration barrier to prevent proteinuria. Podocyte-specific loss of  
373 Vangl2 in mice causes abnormal glomerular maturation in fetal kidneys and increases the  
374 susceptibility of glomerular injury in the adults (Rocque et al., 2015). Thus, Vangl2 play an  
375 important role to promote glomerular development and protect glomerular injury.

376 The improved understanding of PCP proteins in kidney morphogenesis helps to clarify the  
377 link between Wnt/PCP signaling and chronic kidney failure. Nephron, the functional unit of the  
378 kidney, uses numerous ciliated epithelial tubules to reabsorb nutrients and concentrate waste  
379 products. Dysfunctions of primary cilia contribute to the pathogenesis of polycystic kidney disease  
380 (PKD). As Wnt/PCP signaling, PKD genes encoding proteins mainly localized to primary cilia are  
381 also required for oriented cell divisions and CE movements in developing renal tubules, inferring  
382 that defective Wnt/PCP signaling may contribute to PKD as well. However, recent studies  
383 indicate that mutations of PKD genes disrupt renal tubule morphogenesis independently of  
384 Wnt/PCP signaling and that the asymmetric localization of PCP proteins remains intact in adult  
385 cystic kidney (Kunimoto et al., 2017). Moreover, collecting duct-specific loss of Vangl1 and  
386 Vangl2 in mice impairs oriented cell divisions and CE movements, leading to abnormal tubule  
387 diameter in pre-natal renal tubules but not cyst formation in post-natal development (Kunimoto et  
388 al., 2017; Derish et al., 2020). Therefore, PCP proteins play an important role in the accurate  
389 control of tubule lumen diameter. Nevertheless, it remains to be determined in more detail how



390 they regulate early and late stages of kidney epithelial morphogenesis and how they are linked to  
391 other kidney diseases.

### 392 **Inner ear development and hair cell polarity**

393 The inner ear exhibits marvelous features of PCP-dependent asymmetric morphogenesis,  
394 making it an attractive system for studying PCP regulation and function. Mammalian inner ear  
395 consists of a snail-shaped cochlea required for hearing and a vestibular system necessary for  
396 maintaining balance. Cochlear extension and development of the spiral organ of Corti from a  
397 thicker and shorter primordium involve cell intercalations at the luminal surface and directed  
398 migration of hair cells toward the apex (Driver et al., 2017). These highly regulated cellular  
399 processes promote cochlea growth and contribute to the spatial distribution of sensory cells.  
400 Thus, the organ of Corti forms one row of inner hair cells (IHCs) and three rows of outer hair cells  
401 (OHC1, OHC2, and OHC3), which are separated by specialized supporting cells. Based on their  
402 locations with respect to the center of the cochlear spiral, IHCs are referred to as neural/medial  
403 (or proximal), while OHCs are described as abneural/lateral (or distal). Strikingly, both cochlear  
404 and vestibular hair cells display uniformly oriented stereociliary bundles on their apical surfaces.  
405 Wnt/PCP signaling functions to promote cochlea growth and organize the highly choreographed  
406 orientation of stereociliary bundles.

407 In cochlear and vestibular epithelia of the developing mouse embryo, PCP proteins  
408 display striking asymmetric localization in both sensory and supporting cells in a pattern that is  
409 tightly linked to hair cell polarity (Fig. 4A). Fzd3, Fzd6 and Dvl1 accumulate at the neural  
410 boundary of IHCs and OHCs, opposite to the site of stereociliary bundle formation, while Dvl2  
411 and Dvl3 are apparently enriched at the abneural edge (Najarro et al., 2020). Ankrd6 localizes to  
412 the neural edge (Jones et al., 2014). Celsr1 is likely enriched both at the neural side of hair cells  
413 and at the abneural side of supporting cells (Duncan et al., 2017). Analysis by stimulated  
414 emission depletion microscopy indicates that Vangl2 is present at the abneural side of supporting  
415 cells (Giese et al., 2012). Prickle2 is enriched at the neural side of vestibular hair cells before the  
416 formation of stereocilia, and Vangl2 maintains this asymmetric distribution (Deans et al., 2007).

417           Dysfunctions of PCP proteins affect cochlear outgrowth and hair cell polarity. Wnt5a alone  
418 is not sufficient for hair cell polarization in the developing cochlea, but multiple Wnt ligands  
419 collectively contribute to this process (Najarro et al., 2020). During cochlear extension to form the  
420 organ of Corti, Dvl1, Dvl2 and Vangl2 regulate cell intercalation that drives unidirectional  
421 elongation of the primordium. Loss of their functions interferes with outgrowth and  
422 morphogenesis of the cochlea, resulting in abnormal patterning of the cochlear duct and defective  
423 uniform hair bundle orientation (Montcouquiol et al., 2003; Wang et al., 2005). Combined loss of  
424 Fzd3 and Fzd6 mostly affects hair bundle orientation in the organ of Corti (Wang et al., 2006). In  
425 mice, missense mutations that may reduce the structural integrity of Celsr1 protein disrupt the  
426 earliest stages of hair cell polarity in the cochlea and lead to mis-oriented stereociliary bundles  
427 between vestibular hair cells associated with defective vestibular behaviors (Curtin et al., 2003).  
428 Knockout of Fat4 mildly affects hair bundle orientation by mostly leads to defects in cochlear  
429 extension and organization of OHCs, which are exacerbated by reducing the dosage of Fat1  
430 (Saburi et al., 2012).

431           Different PCP genes show genetic interactions in cochlear extension and stereociliary  
432 bundle orientation, likely due to functional redundancy and interdependent asymmetric  
433 localization of their protein products. In particular, there is evidence showing Vangl2 interaction  
434 with other PCP proteins in auditory hair cells by utilizing the *Looptail* mutant. Inhibiting the  
435 secretion of Wnt ligands, including Wnt5a, in a heterozygous *Looptail* background aggravates  
436 defects in cochlear extension and sensory hair cell polarization (Najarro et al., 2020). Loss of  
437 Fzd1 or Fzd2 causes mis-orientations of hair cells only when Vangl2 activity is also reduced (Yu  
438 et al., 2010). Although *Ankrd6* mutant mice show disrupted uniform orientation of hair cells in the  
439 utricle, only *Ankrd6* and *Vangl2* compound mutants display defective hair cell polarity and  
440 patterning in the cochlea (Jones et al., 2014). Fat4 cooperates with Vangl2 to regulate cochlear  
441 elongation and sensory epithelium patterning (Saburi et al., 2012). There are also physical and  
442 genetic interactions between Scrib and Vangl2 in the planar polarization of stereociliary bundles  
443 (Montcouquiol et al., 2003, 2006). It is possible that the *Looptail* mutation contributes partially to

444 enhance hair cell phenotypes because the resulting dysfunctional Vangl2 protein can interfere  
445 with the proper localization of other PCP complexes.

446 During post-natal development, loss of Vangl2 has mild effects on the orientation of  
447 auditory stereociliary bundles and on hearing loss, but mostly causes profound changes in the  
448 shape and distribution of supporting cells that are necessary for cochlear amplification mediated  
449 by OHCs (Copley et al., 2013). Thus, it will be of interest to determine the post-natal requirement  
450 of other PCP proteins in maintaining hearing function.

451 Intriguingly, PCP proteins can function in parallel to instruct hair cell orientation. Zebrafish  
452 lateral line neuromasts also consist of mechanosensory hair cells and support cells. Loss of  
453 Vangl2 directly leads to PCP-dependent defects in hair cells. However, loss of Wnt11 or Fzd7  
454 indirectly affects hair cell polarity by disrupting the alignment of support cells, suggesting a  
455 contribution of support cells in sensory cell orientation (Navajas Acedo et al., 2019). Interestingly,  
456 supporting cells can also dictate hair cell polarization in the mammalian cochlea. The  
457 evolutionarily conserved transmembrane receptor protein tyrosine kinase 7 (PTK7) functions as a  
458 vertebrate-specific PCP regulator. Disruption of PTK7 mostly affects stereociliary bundle  
459 orientation in OHC3 (Lu et al., 2004). Mechanistically, PTK7 acts in parallel with Wnt/PCP  
460 signaling to polarize hair cells by promoting junctional localization of myosin II near the apical  
461 surfaces of supporting cells (Lee et al., 2012). Thus, PTK7 restricts the abnormal positioning of  
462 kinocilia by exerting local tension at the neural edge of hair cells.

463 Cochlear OHCs are innervated by type II spiral ganglion neurons, which project peripheral  
464 axons that extend beyond the IHCs and then turn 90° toward the cochlear base. Disruption of  
465 Wnt secretion suggests that non-canonical Wnts are necessary to trigger Wnt/PCP signaling  
466 during axon guidance (Ghimire and Deans, 2019). Fzd3 and Fzd6 are present at the basolateral  
467 boundary between adjacent supporting cells along the trajectory of axonal growth cones; they  
468 promote the asymmetric localization of Vangl2 and function redundantly to direct cochlear  
469 innervation (Ghimire and Deans, 2019). Consequently, Vangl2 is enriched at intercellular  
470 junctions between cochlear supporting cells and is non-autonomously required for axon turning  
471 (Ghimire et al., 2018). Although it is unclear how Prickle1 and Prickle2 regulate hair cell polarity,

472 Prickle1 is required for neurite outgrowth of type II spiral ganglion neurons (Yang et al., 2017a).  
473 Together, these observations demonstrate an essential role for Wnt/PCP signaling in hair cell  
474 innervation.

475         Generally, dysfunctions of PCP proteins affect the uniform orientation of stereociliary  
476 bundles between neighboring hair cells, but individual hair cells still retain polarized stereocilia  
477 (Fig. 4B). This is because there are independent but nevertheless interconnected mechanisms  
478 coordinating hair cell polarity. Intrinsic or intracellular PCP instructs hair bundle polarization within  
479 a hair cell, while tissue-level or intercellular PCP establishes the uniform orientation of hair cells.  
480 Indeed, several cytoskeletal regulatory proteins, such as Inscuteable (Insc), Partner of  
481 Inscuteable (Pins), Cfp126 and Wdpcp, have been shown to control or restrict positioning of the  
482 tubulin-based kinocilium and arrowhead-shaped distribution of actin-rich stereocilia (Ezan et al.,  
483 2013; Tarchini et al., 2013; Cui et al., 2013; Gegg et al., 2014). Therefore, they can function to  
484 establish intrinsic hair bundle polarity. However, the emergence of asymmetric hair bundle  
485 position in the hair cell apical surface is tightly coupled with long-range orientation cues in the  
486 tissue. Evidence is accumulating that G protein signaling functions to establish intrinsic  
487 asymmetry and interpret intercellular PCP signaling. Accordingly, inhibition of Gai function leads  
488 to randomized positioning of kinocilia and mis-orientations of OHCs (Tarchini et al., 2013). Daple,  
489 a guanine nucleotide exchange factor and a Dvl-binding protein, mediates Wnt-stimulated  
490 heterotrimeric G protein and phosphoinositide 3-kinase signaling to regulate both microtubule-  
491 dependent eccentric kinocilium positioning and asymmetric localization of PCP proteins (Siletti et  
492 al., 2017; Landin Malt et al., 2020). Therefore, a complex interplay between intracellular and  
493 intercellular PCP signaling coordinates the acquisition of hair cell polarity.

#### 494 **Proximal-distal limb outgrowth and elongation**

495         Vertebrate limb buds arise from the lateral plate mesoderm and its overlying ectoderm at  
496 the presumptive forelimb and hindlimb locations. Dynamic formation of cellular protrusion and  
497 biased orientation of cell division are major driving forces that elongate the limb bud along its  
498 proximal-distal axis (Boehm et al., 2010; Wyngaarden et al., 2010). Wnt/PCP signaling plays an  
499 essential role in regulating these directional cell behaviors (Barrow, 2011; Gao and Yang, 2013).

500 Early studies show that *Wnt5a* is expressed in the apical ectoderm ridge (AER) and distal  
501 mesenchyme of the limb bud as a gradient along the proximal-distal axis (Gavin et al., 1990;  
502 Dealy et al., 1993). Similarly, Vangl2 protein also displays a proximal-distal gradient of  
503 asymmetric distribution (Gao et al., 2011).

504         *Wnt5a* plays an important role in establishing cell polarity for limb outgrowth (Fig. 4C).  
505 Mice mutant for *Wnt5a* exhibit reduced individual skeletal elements, with absence of distal  
506 phalanges (Yamaguchi et al., 1999). Analysis of cell behaviors by living imaging in mouse  
507 embryos at E10.5 demonstrate that *Wnt5a* deficiency essentially disrupts the orientation of  
508 mesenchymal cell movements and divisions toward the overlying ectoderm (Gros et al., 2010).  
509 Conversely, implantation of *Wnt5a*-soaked beads into the lateral plate mesoderm of chick  
510 embryos reveals that *Wnt5a* acts as a chemoattractant in the emerging limb bud to instruct  
511 cellular polarization necessary for limb outgrowth (Wyngaarden et al., 2010). Moreover, locally  
512 oriented cell shape changes and biased cell division planes are conserved cellular mechanisms  
513 in vertebrate limb morphogenesis (Wyngaarden et al., 2010).

514         *Wnt5a* promotes the interaction between Ror2 and Vangl2 to establish the asymmetric  
515 localization of Vangl2 in limb chondrocytes (Gao et al., 2011). It acts through Ror2 to induce a  
516 proximal-distal gradient of Vangl2 phosphorylation in the mesenchyme, setting up a higher  
517 Vangl2 activity in most distal cells (Gao et al., 2011). This phosphorylation is mediated by casein  
518 kinase 1 and functions to polarize cellular behaviors of limb chondrocytes in a dose-dependent  
519 manner (Yang et al., 2017b). *Wnt5a* and Vangl2 also show genetic interaction in limb skeletal  
520 development. Reducing *Wnt5a* dosage in *Looptail* mice not only aggravates defects in distal limb  
521 skeletal elements but also causes shortened long bones in the limb, reminiscent of Robinow  
522 syndrome and brachydactyly type B (Wang et al., 2011). Therefore, a *Wnt5a* gradient provides  
523 global cues, which are interpreted by Ror2 and Vangl2, to coordinate directional cellular  
524 behaviors for proximal-distal limb elongation. Interestingly, *Wnt5a* can also generate mechanical  
525 signals to trigger digit elongation likely through ROCK-mediated actomyosin contractility (Parada  
526 et al., 2022). Loss of *Wnt5a* disrupts anisotropic active stresses and CE movements in  
527 developing digits, leading to absence of digit-organizing centers (also known as phalange-forming

528 regions) and digit formation (Parada et al., 2022). Ror2 has been shown to regulate phalange  
529 development mediated by the digit-organizing center (Witte et al., 2010). Thus, Wnt5a may  
530 interact at least partially with Ror2 to combine mechanical cues and molecular signals in digit  
531 emergence.

532 Other PCP proteins also contribute to limb outgrowth. Ryk regulates Wnt/PCP signaling  
533 and limb elongation in part by promoting Vangl2 stability (Andre et al., 2012). Dvl family proteins  
534 are required for Wnt5a-induced Vangl2 phosphorylation by facilitating the interaction of casein  
535 kinase 1 and Vangl2 (Yang et al., 2017b). Mice deficient for Prickle1 show loss of one phalangeal  
536 segment on digits 2-5 in both forelimbs and hindlimbs (Yang et al., 2013; Liu et al., 2014). Thus,  
537 biochemical and functional interactions between PCP proteins are essential for proper limb  
538 morphogenesis.

### 539 **Concluding remarks**

540 PCP proteins contribute to the highly choreographed cellular organization in many  
541 morphogenetic processes. Extensive research has greatly advanced our understanding on their  
542 implications in controlling asymmetric organogenesis and tissue homeostasis. Accumulating  
543 evidence also suggest that dysfunctions of PCP proteins are linked to a variety of human  
544 diseases. Nevertheless, there are still many intriguing questions that deserve further  
545 investigation.

546 Although Wnt ligands can provide global cues to initiate cell polarity in several PCP-  
547 dependent processes, it remains to be determined whether molecular pathways act in concert  
548 with other orientation cues to instruct and establish PCP features. Interestingly, a recent research  
549 shows that the orientation of tissue stretch cooperates with Wnt signaling gradient to align PCP in  
550 *Xenopus* neuroectoderm (Hirano et al., 2022). Since mechanical constraints act as important  
551 cues in planar polarization, it will be important to further develop interdisciplinary approaches for  
552 understanding the interplay of PCP signaling and mechanotransduction in morphogenesis.  
553 Functional gene disruptions combined with in vivo live imaging and manipulation of mechanical  
554 state should help to push the field forward.

555 Another important aspect is to understand how cell polarity can be translated to cell fate  
556 specification. These two processes are clearly interconnected in several contexts, such that  
557 molecular asymmetry provided by PCP proteins helps to promote cell type-specific differentiation.  
558 For example, cell polarity cues are coupled with cell lineage segregation during intestinal stem  
559 cell self-renewal and differentiation (Böttcher et al., 2021). Deciphering the interaction between  
560 molecular signals and mechanical forces in the coupling of cell fate decision and morphogenetic  
561 movements also represents a significant challenge. In this regard, it is noteworthy that Wnt5a  
562 signaling functions in a mechanical feedback that links specification and elongation of developing  
563 digits (Parada et al., 2022).

564 The formation of separately localized “core” PCP protein complexes is important to create  
565 cellular polarization. What are the exact roles of each complex in the coordination of polarized  
566 cellular behaviors? How do they converge to regulate cell polarity? Similarly, it is unclear how and  
567 when the “core” PCP pathway and the Fat/Dchs polarity module coordinate to regulate polarized  
568 cellular behaviors. In *Drosophila*, it appears that they may be coupled by specific Prickle isoforms  
569 through regulation of microtubule plus-end bias (Strutt and Strutt, 2021). Whether this is  
570 conserved in vertebrates awaits future investigation. Therefore, future research using both  
571 invertebrate and vertebrate PCP systems will certainly bring important breakthrough for some of  
572 these issues and provide the link between PCP protein dysfunctions and human diseases.

573

573 **Conflict of interest**

574 The authors declare no competing interests.

575 **Acknowledgments**

576 I would like to apologize for being unable to include many studies in the discussion due to space  
577 limitations. This work was supported by grants from the National Natural Science Foundation of  
578 China (grant number 32070813), the French Muscular Dystrophy Association (AFM-Téléthon  
579 grant number 23545), the Centre National de la Recherche Scientifique (CNRS), and the  
580 Sorbonne University.

581



- 581 **References**
- 582 Adler, P.N., Wallingford, J.B., 2017. From planar cell polarity to ciliogenesis and back: The curious tale of
- 583 the PPE and CPLANE proteins. *Trends Cell Biol.* 27, 379–390.
- 584 Ajima, R., Bisson, J.A., Helt, J.C., Nakaya, M.A., Habas, R., Tessarollo, L., He, X., Morrissey, E.E.,
- 585 Yamaguchi, T.P., Cohen, E.D., 2015. DAAM1 and DAAM2 are co-required for myocardial maturation
- 586 and sarcomere assembly. *Dev. Biol.* 408, 126–139.
- 587 Andre, P., Wang, Q., Wang, N., Gao, B., Schilit, A., Halford, M.M., Stacker, S.A., Zhang, X., Yang, Y.,
- 588 2012. The Wnt coreceptor Ryk regulates Wnt/planar cell polarity by modulating the degradation of the
- 589 core planar cell polarity component Vangl2. *J. Biol. Chem.* 287, 44518–44525.
- 590 Antic, D., Stubbs, J.L., Suyama, K., Kintner, C., Scott, M.P., Axelrod, J.D., 2010. Planar cell polarity
- 591 enables posterior localization of nodal cilia and left-right axis determination during mouse and *Xenopus*
- 592 embryogenesis. *PLoS One* 5, e8999.
- 593 Axelrod, J.D., 2020. Planar cell polarity signaling in the development of left-right asymmetry. *Curr. Opin.*
- 594 *Cell Biol.* 62, 61–69.
- 595 Bagherie-Lachidan, M., Reginensi, A., Pan, Q., Zaveri, H.P., Scott, D.A., Blencowe, B.J., Helmbacher, F.,
- 596 McNeill, H., 2015. Stromal Fat4 acts non-autonomously with Dchs1/2 to restrict the nephron progenitor
- 597 pool. *Development* 142, 2564–2573.
- 598 Barrow, J., 2011. Wnt/planar cell polarity signaling: an important mechanism to coordinate growth and
- 599 patterning in the limb. *Organogenesis* 7, 260–266.
- 600 Bellchambers, H.M., Ware, S.M., 2021. Loss of *Zic3* impairs planar cell polarity leading to abnormal left-
- 601 right signaling, heart defects and neural tube defects. *Hum. Mol. Genet.* 30, 2402–2415.
- 602 Blair, S., McNeill, H., 2018. Big roles for Fat cadherins. *Curr. Opin. Cell Biol.* 51, 73–80.
- 603 Boehm, B., Westerberg, H., Lesnicar-Pucko, G., Raja, S., Rautschka, M., Cotterell, J., Swoger, J., Sharpe,
- 604 J., 2010. The role of spatially controlled cell proliferation in limb bud morphogenesis. *PLoS Biol.* 8,
- 605 e1000420.
- 606 Borovina, A., Superina, S., Voskas, D., Ciruna, B., 2010. Vangl2 directs the posterior tilting and asymmetric
- 607 localization of motile primary cilia. *Nat. Cell Biol.* 12, 407–412.
- 608 Böttcher, A., Büttner, M., Tritschler, S., Sterr, M., Aliluev, A., Oppenländer, L., Burtscher, I., Sass, S.,
- 609 Irmiler, M., Beckers, J., et al., 2021. Non-canonical Wnt/PCP signalling regulates intestinal stem cell
- 610 lineage priming towards enteroendocrine and Paneth cell fates. *Nat. Cell Biol.* 23, 23–31.
- 611 Brzóska, H.Ł., d'Esposito, A.M., Kolatsi-Joannou, M., Patel, V., Igarashi, P., Lei, Y., Finnell, R.H., Lythgoe,
- 612 M.F., Woolf, A.S., Papakrivopoulou, E., et al., 2016. Planar cell polarity genes *Celsr1* and *Vangl2* are
- 613 necessary for kidney growth, differentiation, and rostrocaudal patterning. *Kidney Int.* 90, 1274–1284.
- 614 Carroll, T.J., Yu, J., 2012. The kidney and planar cell polarity. *Curr. Top. Dev. Biol.* 101, 185–212.
- 615 Cervantes, S., Yamaguchi, T.P., Hebrok, M., 2009. *Wnt5a* is essential for intestinal elongation in mice.
- 616 *Dev. Biol.* 326, 285–294.
- 617 Cheong, S.S., Akram, K.M., Matellan, C., Kim, S.Y., Gaboriau, D.C.A., Hind, M., Del Río Hernández, A.E.,
- 618 Griffiths, M., Dean, C.H., 2020. The planar polarity component VANGL2 is a key regulator of
- 619 mechanosignaling. *Front. Cell Dev. Biol.* 8, 577201.
- 620 Chu, C.W., Ossipova, O., Ioannou, A., Sokol, S.Y., 2016. Prickle3 synergizes with *Wtip* to regulate basal
- 621 body organization and cilia growth. *Sci. Rep.* 6, 24104.
- 622 Copley, C.O., Duncan, J.S., Liu, C., Cheng, H., Deans, M.R., 2013. Postnatal refinement of auditory hair
- 623 cell planar polarity deficits occurs in the absence of *Vangl2*. *J. Neurosci.* 33, 14001–14016.
- 624 Cui, C., Chatterjee, B., Lozito, T.P., Zhang, Z., Francis, R.J., Yagi, H., Swanhart, L.M., Sanker, S., Francis,
- 625 D., Yu, Q., et al., 2013. *Wdpcp*, a PCP protein required for ciliogenesis, regulates directional cell
- 626 migration and cell polarity by direct modulation of the actin cytoskeleton. *PLoS Biol.* 11, e1001720.
- 627 Curtin, J.A., Quint, E., Tsipouri, V., Arkell, R.M., Cattanch, B., Copp, A.J., Henderson, D.J., Spurr, N.,
- 628 Stanier, P., Fisher, E.M., et al., 2003. Mutation of *Celsr1* disrupts planar polarity of inner ear hair cells
- 629 and causes severe neural tube defects in the mouse. *Curr. Biol.* 13, 1129–1133.
- 630 Das, A., Tanigawa, S., Karner, C.M., Xin, M., Lum, L., Chen, C., Olson, E.N., Perantoni, A.O., Carroll, T.J.,
- 631 2013. Stromal-epithelial crosstalk regulates kidney progenitor cell differentiation. *Nat. Cell Biol.* 15,
- 632 1035–1044.
- 633 Dealy, C.N., Roth, A., Ferrari, D., Brown, A.M., Kosher, R.A., 1993. *Wnt-5a* and *Wnt-7a* are expressed in
- 634 the developing chick limb bud in a manner suggesting roles in pattern formation along the proximodistal
- 635 and dorsoventral axes. *Mech. Dev.* 43, 175–186.
- 636 Deans, M.R., Antic, D., Suyama, K., Scott, M.P., Axelrod, J.D., Goodrich, L.V., 2007. Asymmetric
- 637 distribution of prickle-like 2 reveals an early underlying polarization of vestibular sensory epithelia in the
- 638 inner ear. *J. Neurosci.* 27, 3139–3147.

639 Derish, I., Lee, J.K.H., Wong-King-Cheong, M., Babayeva, S., Caplan, J., Leung, V., Shahinian, C., Gravel,  
640 M., Deans, M.R., Gros, P., et al., 2020. Differential role of planar cell polarity gene *Vangl2* in embryonic  
641 and adult mammalian kidneys. *PLoS One* 15, e0230586.

642 Derrick, C.J., Santos-Ledo, A., Eley, L., Henderson, D.J., Chaudhry, B., 2022. Sequential action of *jnk*  
643 genes establishes the embryonic left-right axis. *Development* 149, dev200136.

644 Descamps, B., Sewduth, R., Ferreira Tojais, N., Jaspard, B., Reynaud, A., Sohet, F., Lacolley, P., Allières,  
645 C., Lamazière, J.M., Moreau, C., et al., 2012. Frizzled 4 regulates arterial network organization through  
646 noncanonical Wnt/planar cell polarity signaling. *Circ. Res.* 110, 47–58.

647 Desgrange, A., Le Garrec, J.F., Meilhac, S.M., 2018. Left-right asymmetry in heart development and  
648 disease: forming the right loop. *Development* 145, dev162776.

649 Driver, E.C., Northrop, A., Kelley, M.W., 2017. Cell migration, intercalation and growth regulate mammalian  
650 cochlear extension. *Development* 144, 3766–3776.

651 Duncan, J.S., Stoller, M.L., Francl, A.F., Tissir, F., Devenport, D., Deans, M.R., 2017. *Celsr1* coordinates  
652 the planar polarity of vestibular hair cells during inner ear development. *Dev. Biol.* 423, 126–137.

653 Dush, M.K., Nascone-Yoder, N.M., 2019. *Vangl2* coordinates cell rearrangements during gut elongation.  
654 *Dev. Dyn.* 248, 569–582.

655 Ezan, J., Lasvaux, L., Gezer, A., Novakovic, A., May-Simera, H., Belotti, E., Lhoumeau, A.C., Birnbaumer,  
656 L., Beer-Hammer, S., Borg, J.P., et al., 2013. Primary cilium migration depends on G-protein signalling  
657 control of subapical cytoskeleton. *Nat. Cell Biol.* 15, 1107–1115.

658 Gao, B., Song, H., Bishop, K., Elliot, G., Garrett, L., English, M.A., Andre, P., Robinson, J., Sood, R.,  
659 Minami, Y., et al., 2011. Wnt signaling gradients establish planar cell polarity by inducing *Vangl2*  
660 phosphorylation through *Ror2*. *Dev. Cell* 20, 163–176.

661 Gao, B., Yang, Y., 2013. Planar cell polarity in vertebrate limb morphogenesis. *Curr. Opin. Genet. Dev.* 23,  
662 438–444.

663 Gavin, B.J., McMahon, J.A., McMahon, A.P., 1990. Expression of multiple novel Wnt-1/int-1-related genes  
664 during fetal and adult mouse development. *Genes Dev.* 4, 2319–2332.

665 Gegg, M., Böttcher, A., Burtscher, I., Hasenoeder, S., Van Campenhout, C., Aichler, M., Walch, A., Grant,  
666 S.G., Lickert, H., 2014. Flattop regulates basal body docking and positioning in mono- and multiciliated  
667 cells. *Elife* 3, e03842.

668 Ghimire, S.R., Deans, M.R., 2019. Frizzled3 and frizzled6 cooperate with *Vangl2* to direct cochlear  
669 innervation by type II spiral ganglion neurons. *J. Neurosci.* 39, 8013–8023.

670 Ghimire, S.R., Ratzan, E.M., Deans, M.R., 2018. A non-autonomous function of the core PCP protein  
671 *VANGL2* directs peripheral axon turning in the developing cochlea. *Development* 145, dev159012.

672 Gibbs, B.C., Damerla, R.R., Vldar, E.K., Chatterjee, B., Wan, Y., Liu, X., Cui, C., Gabriel, G.C., Zahid, M.,  
673 Yagi, H., et al., 2016. Prickle1 mutation causes planar cell polarity and directional cell migration defects  
674 associated with cardiac outflow tract anomalies and other structural birth defects. *Biol. Open* 5, 323–  
675 335.

676 Giese, A.P., Ezan, J., Wang, L., Lasvaux, L., Lembo, F., Mazzocco, C., Richard, E., Reboul, J., Borg, J.P.,  
677 Kelley, M.W., et al., 2012. *Gipc1* has a dual role in *Vangl2* trafficking and hair bundle integrity in the  
678 inner ear. *Development* 139, 3775–3785.

679 Grimes, D.T., Burdine, R.D., 2017. Left-right patterning: Breaking symmetry to asymmetric morphogenesis.  
680 *Trends Genet.* 33, 616–628.

681 Gros, J., Hu, J.K., Vinegoni, C., Feruglio, P.F., Weissleder, R., Tabin, C.J., 2010. WNT5A/JNK and  
682 FGF/MAPK pathways regulate the cellular events shaping the vertebrate limb bud. *Curr. Biol.* 1993–  
683 2002.

684 Grzymkowski, J., Wyatt, B., Nascone-Yoder, N., 2020. The twists and turns of left-right asymmetric gut  
685 morphogenesis. *Development* 147, dev187583.

686 Gubb, D., García-Bellido, A., 1982. A genetic analysis of the determination of cuticular polarity during  
687 development in *Drosophila melanogaster*. *J. Embryol. Exp. Morphol.* 68, 37–57.

688 Hashimoto, M., Shinohara, K., Wang, J., Ikeuchi, S., Yoshida, S., Meno, C., Nonaka, S., Takada, S., Hatta,  
689 K., Wynshaw-Boris, A., et al., 2010. Planar polarization of node cells determines the rotational axis of  
690 node cilia. *Nat. Cell Biol.* 12, 170–176.

691 Henderson, D.J., Long, D.A., Dean, C.H., 2018. Planar cell polarity in organ formation. *Curr. Opin. Cell*  
692 *Biol.* 55, 96–103.

693 Henderson, D.J., Phillips, H.M., Chaudhry, B., 2006. Vang-like 2 and noncanonical Wnt signaling in outflow  
694 tract development. *Trends Cardiovasc. Med.* 16, 38–45.

695 Hirano, S., Mii, Y., Charras, G., Michiue, T., 2022. Alignment of cell long axis by unidirectional tension acts  
696 cooperatively with Wnt signalling to establish PCP. *Development* 149, dev.200515.

697 Huycke, T.R., Tabin, C.J., 2018. Chick midgut morphogenesis. *Int. J. Dev. Biol.* 62, 109–119.

698 Jones, C., Qian, D., Kim, S.M., Li, S., Ren, D., Knapp, L., Sprinzak, D., Avraham, K.B., Matsuzaki, F., Chi,  
699 F., et al., 2014. Ankrd6 is a mammalian functional homolog of *Drosophila* planar cell polarity gene *diego*  
700 and regulates coordinated cellular orientation in the mouse inner ear. *Dev. Biol.* 395, 62–72.

701 Juan, T., Géminard, C., Coutelis, J.B., Cerezo, D., Polès, S., Noselli, S., Fürthauer, M., 2018. Myosin1D is  
702 an evolutionarily conserved regulator of animal left-right asymmetry. *Nat. Commun.* 9, 1942.

703 Kadzik, R.S., Cohen, E.D., Morley, M.P., Stewart, K.M., Lu, M.M., Morrisey, E.E., 2014. Wnt ligand/Frizzled  
704 2 receptor signaling regulates tube shape and branch-point formation in the lung through control of  
705 epithelial cell shape. *Proc. Natl. Acad. Sci. U. S. A.* 111, 12444–12449x.

706 Karner, C.M., Chirumamilla, R., Aoki, S., Igarashi, P., Wallingford, J.B., Carroll, T.J., 2009. Wnt9b signaling  
707 regulates planar cell polarity and kidney tubule morphogenesis. *Nat. Genet.* 41, 793–799.

708 Kishimoto, K., Tamura, M., Nishita, M., Minami, Y., Yamaoka, A., Abe, T., Shigeta, M., Morimoto, M., 2018.  
709 Synchronized mesenchymal cell polarization and differentiation shape the formation of the murine  
710 trachea and esophagus. *Nat. Commun.* 9, 2816.

711 Kispert, A., Vainio, S., McMahon, A.P., 1998. Wnt-4 is a mesenchymal signal for epithelial transformation of  
712 metanephric mesenchyme in the developing kidney. *Development* 125, 4225–4234.

713 Krneta-Stankic, V., Corkins, M.E., Paulucci-Holthausen, A., Kloc, M., Gladden, A.B., Miller, R.K., 2021. The  
714 Wnt/PCP formin Daam1 drives cell-cell adhesion during nephron development. *Cell Rep.* 36, 109340.

715 Kunimoto, K., Bayly, R.D., Vladar, E.K., Vonderfecht, T., Gallagher, A.R., Axelrod, J.D., 2017. Disruption of  
716 core planar cell polarity signaling regulates renal tubule morphogenesis but is not cystogenic. *Curr. Biol.*  
717 27, 3120–3131.e4.

718 Landin Malt, A., Hogan, A.K., Smith, C.D., Madani, M.S., Lu, X., 2020. Wnts regulate planar cell polarity via  
719 heterotrimeric G protein and PI3K signaling. *J. Cell Biol.* 219, e201912071.

720 Lavalou, J., Lecuit, T., 2022. In search of conserved principles of planar cell polarization. *Curr. Opin.*  
721 *Genet. Dev.* 72, 69–81.

722 Lawrence, P.A., Shelton, P.M., 1975. The determination of polarity in the developing insect retina. *J.*  
723 *Embryol. Exp. Morphol.* 33, 471–486.

724 Lee, H.J., Shi, D.L., Zheng, J.J., 2015. Conformational change of Dishevelled plays a key regulatory role in  
725 the Wnt signaling pathways. *Elife* 4, e08142.

726 Lee, J., Andreeva, A., Sipe, C.W., Liu, L., Cheng, A., Lu, X., 2012. PTK7 regulates myosin II activity to  
727 orient planar polarity in the mammalian auditory epithelium. *Curr. Biol.* 22, 956–966.

728 Li, C., Smith, S.M., Peinado, N., Gao, F., Li, W., Lee, M.K., Zhou, B., Bellusci, S., Pryhuber, G.S., Ho, H.H.,  
729 et al., 2020. WNT5a-ROR signaling is essential for alveologenesis. *Cells* 9, 384.

730 Li, D., Angermeier, A., Wang, J., 2019. Planar cell polarity signaling regulates polarized second heart field  
731 morphogenesis to promote both arterial and venous pole septation. *Development* 146, dev181719.

732 Li, D., Hallett, M.A., Zhu, W., Rubart, M., Liu, Y., Yang, Z., Chen, H., Haneline, L.S., Chan, R.J., Schwartz,  
733 R.J., et al., 2011. Dishevelled-associated activator of morphogenesis 1 (Daam1) is required for heart  
734 morphogenesis. *Development* 138, 303–315.

735 Lienkamp, S.S., Liu, K., Karner, C.M., Carroll, T.J., Ronneberger, O., Wallingford, J.B., Walz, G., 2012.  
736 Vertebrate kidney tubules elongate using a planar cell polarity-dependent, rosette-based mechanism of  
737 convergent extension. *Nat. Genet.* 44, 1382–1387.

738 Little, R.B., Norris, D.P., 2021. Right, left and cilia: How asymmetry is established. *Semin. Cell Dev. Biol.*  
739 110, 11–18.

740 Liu, C., Lin, C., Gao, C., May-Simera, H., Swaroop, A., Li, T., 2014. Null and hypomorph Prickle1 alleles in  
741 mice phenocopy human Robinow syndrome and disrupt signaling downstream of Wnt5a. *Biol. Open* 3,  
742 861–870.

743 Loscertales, M., Mikels, A.J., Hu, J.K., Donahoe, P.K., Roberts, D.J., 2008. Chick pulmonary Wnt5a directs  
744 airway and vascular tubulogenesis. *Development* 135, 1365–1376.

745 Lu, X., Borchers, A.G., Jolicoeur, C., Rayburn, H., Baker, J.C., Tessier-Lavigne, M., 2004. PTK7/CCK-4 is  
746 a novel regulator of planar cell polarity in vertebrates. *Nature* 430, 93–98.

747 Mao, Y., Francis-West, P., Irvine, K.D., 2015. Fat4/Dchs1 signaling between stromal and cap mesenchyme  
748 cells influences nephrogenesis and ureteric bud branching. *Development* 142, 2574–2585.

749 Matsuyama, M., Aizawa, S., Shimono, A., 2009. Sfrp controls apicobasal polarity and oriented cell division  
750 in developing gut epithelium. *PLoS Genet.* 5, e1000427.

751 May-Simera, H., Kelley, M.W., 2012. Planar cell polarity in the inner ear. *Curr. Top. Dev. Biol.* 101, 111–  
752 140.

753 Merks, A.M., Swinarski, M., Meyer, A.M., Müller, N.V., Özcan, I., Donat, S., Burger, A., Gilbert, S.,  
754 Mosimann, C., Abdelilah-Seyfried, S., et al., 2018. Planar cell polarity signalling coordinates heart tube  
755 remodelling through tissue-scale polarisation of actomyosin activity. *Nat. Commun.* 9, 2161.

756 Milgrom-Hoffman, M., Humbert, P.O., 2018. Regulation of cellular and PCP signalling by the Scribble  
757 polarity module. *Semin. Cell Dev. Biol.* 81, 33–45.

758 Miller, R.K., Canny, S.G., Jang, C.W., Cho, K., Ji, H., Wagner, D.S., Jones, E.A., Habas, R., McCrea, P.D.,  
759 2011. Pronephric tubulogenesis requires Daam1-mediated planar cell polarity signaling. *J. Am. Soc.*  
760 *Nephrol.* 22, 1654–1664.

761 Minegishi, K., Hashimoto, M., Ajima, R., Takaoka, K., Shinohara, K., Ikawa, Y., Nishimura, H., McMahon,  
762 A.P., Willert, K., Okada, Y., et al., 2017. A Wnt5 activity asymmetry and intercellular signaling via PCP  
763 proteins polarize node cells for left-right symmetry breaking. *Dev. Cell* 40, 439–452.e4.

764 Montcouquiol, M., Rachel, R.A., Lanford, P.J., Copeland, N.G., Jenkins, N.A., Kelley, M.W., 2003.  
765 Identification of *Vangl2* and *Scrb1* as planar polarity genes in mammals. *Nature* 423, 173–177.

766 Montcouquiol, M., Sans, N., Huss, D., Kach, J., Dickman, J.D., Forge, A., Rachel, R.A., Copeland, N.G.,  
767 Jenkins, N.A., Bogani, D., et al., 2006. Asymmetric localization of *Vangl2* and *Fz3* indicate novel  
768 mechanisms for planar cell polarity in mammals. *J. Neurosci.* 26, 5265–5275.

769 Najarro, E.H., Huang, J., Jacobo, A., Quiruz, L.A., Grillet, N., Cheng, A.G., 2020. Dual regulation of planar  
770 polarization by secreted Wnts and *Vangl2* in the developing mouse cochlea. *Development* 147,  
771 dev191981.

772 Navajas Acedo, J., Voas, M.G., Alexander, R., Woolley, T., Unruh, J.R., Li, H., Moens, C., Piotrowski, T.,  
773 2019. PCP and Wnt pathway components act in parallel during zebrafish mechanosensory hair cell  
774 orientation. *Nat. Commun.* 10, 3993.

775 Nishita, M., Qiao, S., Miyamoto, M., Okinaka, Y., Yamada, M., Hashimoto, R., Iijima, K., Otani, H.,  
776 Hartmann, C., Nishinakamura, R., et al., 2014. Role of *Wnt5a-Ror2* signaling in morphogenesis of the  
777 metanephric mesenchyme during ureteric budding. *Mol. Cell. Biol.* 34, 3096–3105.

778 O'Brien, L.L., Combes, A.N., Short, K.M., Lindström, N.O., Whitney, P.H., Cullen-McEwen, L.A., Ju, A.,  
779 Abdelhalim, A., Michos, O., Bertram, J.F., et al., 2018. *Wnt11* directs nephron progenitor polarity and  
780 motile behavior ultimately determining nephron endowment. *Elife* 7, e40392.

781 Parada, C., Banavar, S.P., Khalilian, P., Rigaud, S., Michaut, A., Liu, Y., Joshy, D.M., Campàs, O., Gros,  
782 J., 2022. Mechanical feedback defines organizing centers to drive digit emergence. *Dev. Cell* 57, 854–  
783 866.e6.

784 Phillips, H.M., Hildreth, V., Peat, J.D., Murdoch, J.N., Kobayashi, K., Chaudhry, B., Henderson, D.J., 2008.  
785 Non-cell-autonomous roles for the planar cell polarity gene *Vangl2* in development of the coronary  
786 circulation. *Circ. Res.* 102, 615–623.

787 Phillips, H.M., Murdoch, J.N., Chaudhry, B., Copp, A.J., Henderson, D.J., 2005. *Vangl2* acts via RhoA  
788 signaling to regulate polarized cell movements during development of the proximal outflow tract. *Circ.*  
789 *Res.* 96, 292–299.

790 Poobalasingam, T., Yates, L.L., Walker, S.A., Pereira, M., Gross, N.Y., Ali, A., Kolatsi-Joannou, M.,  
791 Jarvelin, M.R., Pekkanen, J., Papakrivopoulou, E., et al., 2017. Heterozygous *Vangl2*(Looptail) mice  
792 reveal novel roles for the planar cell polarity pathway in adult lung homeostasis and repair. *Dis. Model*  
793 *Mech.* 10, 409–423.

794 Ramsbottom, S.A., Sharma, V., Rhee, H.J., Eley, L., Phillips, H.M., Rigby, H.F., Dean, C., Chaudhry, B.,  
795 Henderson, D.J., 2014. *Vangl2*-regulated polarisation of second heart field-derived cells is required for  
796 outflow tract lengthening during cardiac development. *PLoS Genet.* 10, e1004871.

797 Rao-Bhatia, A., Zhu, M., Yin, W.C., Coquenlorge, S., Zhang, X., Woo, J., Sun, Y., Dean, C.H., Liu, A., Hui,  
798 C.C., et al., 2020. Hedgehog-activated *Fat4* and PCP pathways mediate mesenchymal cell clustering  
799 and villus formation in gut development. *Dev. Cell* 52, 647–658.e6.

800 Rocque, B.L., Babayeva, S., Li, J., Leung, V., Nezvitsky, L., Cybulsky, A.V., Gros, P., Torban, E., 2015.  
801 Deficiency of the planar cell polarity protein *Vangl2* in podocytes affects glomerular morphogenesis and  
802 increases susceptibility to injury. *J. Am. Soc. Nephrol.* 26, 576–586.

803 Saburi, S., Hester, I., Fischer, E., Pontoglio, M., Eremina, V., Gessler, M., Quaggin, S.E., Harrison, R.,  
804 Mount, R., McNeill, H., 2008. Loss of *Fat4* disrupts PCP signaling and oriented cell division and leads to  
805 cystic kidney disease. *Nat. Genet.* 40, 1010–1015.

806 Saburi, S., Hester, I., Goodrich, L., McNeill, H., 2012. Functional interactions between *Fat* family cadherins  
807 in tissue morphogenesis and planar polarity. *Development* 139, 1806–1820.

808 Sai, X., Ikawa, Y., Nishimura, H., Mizuno, K., Kajikawa, E., Katoh, T.A., Kimura, T., Shiratori, H., Takaoka,  
809 K., Hamada, H., et al., 2022. Planar cell polarity-dependent asymmetric organization of microtubules for  
810 polarized positioning of the basal body in node cells. *Development* 149, dev200315.

811 Savin, T., Kurpios, N.A., Shyer, A.E., Florescu, P., Liang, H., Mahadevan, L., Tabin, C.J., 2011. On the  
812 growth and form of the gut. *Nature* 476, 57–62.

813 Shi, D.L., 2020. Decoding Dishevelled-mediated Wnt signaling in vertebrate early development. *Front. Cell*  
814 *Dev. Biol.* 8, 588370.

815 Shoshkes-Carmel, M., Wang, Y.J., Wangenstein, K.J., Tóth, B., Kondo, A., Massasa, E.E., Itzkovitz, S.,  
816 Kaestner, K.H., 2018. Subepithelial telocytes are an important source of Wnts that supports intestinal  
817 crypts. *Nature* 557, 242–246.

818 Siletti, K., Tarchini, B., Hudspeth, A.J., 2017. Duple coordinates organ-wide and cell-intrinsic polarity to  
819 pattern inner-ear hair bundles. *Proc. Natl. Acad. Sci. U. S. A.* 114, E11170–E11179.

820 Sinha, T., Li, D., Théveniau-Ruissy, M., Hutson, M.R., Kelly, R.G., Wang, J., 2015. Loss of *Wnt5a* disrupts  
821 second heart field cell deployment and may contribute to OFT malformations in DiGeorge syndrome.  
822 *Hum. Mol. Genet.* 24, 1704–1716.

823 Sinha, T., Wang, B., Evans, S., Wynshaw-Boris, A., Wang, J., 2012. Disheveled mediated planar cell  
824 polarity signaling is required in the second heart field lineage for outflow tract morphogenesis. *Dev. Biol.*  
825 370, 135–144.

826 Skouloudaki, K., Puetz, M., Simons, M., Courbard, J.R., Boehlke, C., Hartleben, B., Engel, C., Moeller,  
827 M.J., Englert, C., Bollig, F., et al., 2009. Scribble participates in Hippo signaling and is required for  
828 normal zebrafish pronephros development. *Proc. Natl. Acad. Sci. U. S. A.* 106, 8579–8584.

829 Song, H., Hu, J., Chen, W., Elliott, G., Andre, P., Gao, B., Yang, Y., 2010. Planar cell polarity breaks  
830 bilateral symmetry by controlling ciliary positioning. *Nature* 466, 378–382.

831 Stark, K., Vainio, S., Vassileva, G., McMahon, A.P., 1994. Epithelial transformation of metanephric  
832 mesenchyme in the developing kidney regulated by *Wnt-4*. *Nature* 372, 679–683.

833 Strutt, H., Strutt, D., 2021. How do the Fat-Dachsous and core planar polarity pathways act together and  
834 independently to coordinate polarized cell behaviours? *Open Biol.* 11, 200356.

835 Tarchini, B., Jolicoeur, C., Cayouette, M., 2013. A molecular blueprint at the apical surface establishes  
836 planar asymmetry in cochlear hair cells. *Dev. Cell* 27, 88–102.

837 Tingler, M., Kurz, S., Maerker, M., Ott, T., Fuhl, F., Schweickert, A., LeBlanc-Straceski, J.M., Noselli, S.,  
838 Blum, M., 2018. A conserved role of the unconventional Myosin 1d in laterality determination. *Curr. Biol.*  
839 28, 810–816.e3.

840 Torban, E., Sokol, S.Y., 2021. Planar cell polarity pathway in kidney development, function and disease.  
841 *Nat. Rev. Nephrol.* 17, 369–385.

842 Vadar, E.K., Bayly, R.D., Sangoram, A.M., Scott, M.P., Axelrod, J.D., 2012. Microtubules enable the planar  
843 cell polarity of airway cilia. *Curr. Biol.* 22, 2203–2212.

844 Vadar, E.K., Königshoff, M., 2020. Noncanonical *Wnt* planar cell polarity signaling in lung development  
845 and disease. *Biochem. Soc. Trans.* 48, 231–243.

846 Vadar, E.K., Nayak, J.V., Milla, C.E., Axelrod, J.D., 2016. Airway epithelial homeostasis and planar cell  
847 polarity signaling depend on multiciliated cell differentiation. *JCI Insight* 1, e88027.

848 Wallingford, J.B., 2012. Planar cell polarity and the developmental control of cell behavior in vertebrate  
849 embryos. *Annu. Rev. Cell Dev. Biol.* 28, 627–653.

850 Wang, B., Sinha, T., Jiao, K., Serra, R., Wang, J., 2011. Disruption of PCP signaling causes limb  
851 morphogenesis and skeletal defects and may underlie Robinow syndrome and brachydactyly type B.  
852 *Hum. Mol. Genet.* 20, 271–285.

853 Wang, I.Y., Chung, C.F., Babayeva, S., Sogomonian, T., Torban E., 2021. Loss of planar cell polarity  
854 effector Fuzzy causes renal hypoplasia by disrupting several signaling pathways. *J. Dev. Biol.* 10, 1.

855 Wang, J., Mark, S., Zhang, X., Qian, D., Yoo, S.J., Radde-Gallwitz, K., Zhang, Y., Lin, X., Collazo, A.,  
856 Wynshaw-Boris, A., et al., 2005. Regulation of polarized extension and planar cell polarity in the cochlea  
857 by the vertebrate PCP pathway. *Nat. Genet.* 37, 980–985.

858 Wang, M., Marco, P., Capra, V., Kibar, Z., 2019. Update on the role of the non-canonical *Wnt*/planar cell  
859 polarity pathway in neural tube defects. *Cells* 8, 1198.

860 Wang, S., Cebrian, C., Schnell, S., Gumucio, D.L., 2018. Radial *WNT5A*-guided post-mitotic filopodial  
861 pathfinding is critical for midgut tube elongation. *Dev. Cell* 46, 173–188.e3.

862 Wang, S., Roy, J.P., Tomlinson, A.J., Wang, E.B., Tsai, Y.H., Cameron, L., Underwood, J., Spence, J.R.,  
863 Walton, K.D., Stacker, S.A., et al., 2020. RYK-mediated filopodial pathfinding facilitates midgut  
864 elongation. *Development* 147, dev195388.

865 Wang, Y., Guo, N., Nathans, J., 2006. The role of *Frizzled3* and *Frizzled6* in neural tube closure and in the  
866 planar polarity of inner ear sensory hair cells. *J. Neurosci.* 26, 2147–2156.

867 Welsh, I.C., Thomsen, M., Gludish, D.W., Alfonso-Parra, C., Bai, Y., Martin, J.F., Kurpios, N.A., 2013.  
868 Integration of left-right *Pitx2* transcription and *Wnt* signaling drives asymmetric gut morphogenesis via  
869 *Daam2*. *Dev. Cell* 26, 629–644.

870 Witte, F., Chan, D., Economides, A.N., Mundlos, S., Stricker, S., 2010. Receptor tyrosine kinase-like  
871 orphan receptor 2 (ROR2) and Indian hedgehog regulate digit outgrowth mediated by the phalanx-  
872 forming region. *Proc. Natl. Acad. Sci. U. S. A.* 107, 14211–14216.

873 Wyngaarden, L.A., Vogelii, K.M., Ciruna, B.G., Wells, M., Hadjantonakis, A.K., Hopyan, S., 2010. Oriented  
874 cell motility and division underlie early limb bud morphogenesis. *Development* 137, 2551–2558.

875 Yamaguchi, T.P., Bradley, A., McMahon, A.P., Jones, S., 1999. A *Wnt5a* pathway underlies outgrowth of  
876 multiple structures in the vertebrate embryo. *Development* 126, 1211–1223.

877 Yang, T., Bassuk, A.G., Fritsch, B., 2013. Prickle1 stunts limb growth through alteration of cell polarity and  
878 gene expression. *Dev. Dyn.* 242, 1293–1306.

879 Yang, T., Kersigo, J., Wu, S., Fritsch, B., Bassuk, A.G., 2017a. Prickle1 regulates neurite outgrowth of  
880 apical spiral ganglion neurons but not hair cell polarity in the murine cochlea. *PLoS One* 12, e0183773.

881 Yang, W., Garrett, L., Feng, D., Elliott, G., Liu, X., Wang, N., Wong, Y.M., Choi, N.T., Yang, Y., Gao, B.,  
882 2017b. Wnt-induced Vangl2 phosphorylation is dose-dependently required for planar cell polarity in  
883 mammalian development. *Cell Res.* 27, 1466–1484.

884 Yang, Y., Mlodzik, M., 2015. Wnt-Frizzled/planar cell polarity signaling: cellular orientation by facing the  
885 wind (Wnt). *Annu. Rev. Cell Dev. Biol.* 31, 623–646.

886 Yates, L.L., Papakrivopoulou, J., Long, D.A., Goggolidou, P., Connolly, J.O., Woolf, A.S., Dean, C.H.,  
887 2010a. The planar cell polarity gene Vangl2 is required for mammalian kidney-branching  
888 morphogenesis and glomerular maturation. *Hum. Mol. Genet.* 19, 4663–4676.

889 Yates, L.L., Schnatwinkel, C., Hazelwood, L., Chessum, L., Paudyal, A., Hilton, H., Romero, M.R., Wilde,  
890 J., Bogani, D., Sanderson, J., et al., 2013. Scribble is required for normal epithelial cell-cell contacts and  
891 lumen morphogenesis in the mammalian lung. *Dev. Biol.* 373, 267–280.

892 Yates, L.L., Schnatwinkel, C., Murdoch, J.N., Bogani, D., Formstone, C.J., Townsend, S., Greenfield, A.,  
893 Niswander, L.A., Dean, C.H., 2010b. The PCP genes *Celsr1* and *Vangl2* are required for normal lung  
894 branching morphogenesis. *Hum. Mol. Genet.* 19, 2251–2267.

895 Ye, X., Wang, Y., Rattner, A., Nathans, J., 2011. Genetic mosaic analysis reveals a major role for frizzled 4  
896 and frizzled 8 in controlling ureteric growth in the developing kidney. *Development* 138, 1161–1172.

897 Yu, H., Smallwood, P.M., Wang, Y., Vidaltamayo, R., Reed, R., Nathans, J., 2010. Frizzled 1 and frizzled 2  
898 genes function in palate, ventricular septum and neural tube closure: general implications for tissue  
899 fusion processes. *Development* 137, 3707–3717.

900 Yu, H., Ye, X., Guo, N., Nathans, J., 2012. Frizzled 2 and frizzled 7 function redundantly in convergent  
901 extension and closure of the ventricular septum and palate: evidence for a network of interacting genes.  
902 *Development* 139, 4383–4394.

903 Yuan, K., Shamskhov, E.A., Orcholski, M.E., Nathan, A., Reddy, S., Honda, H., Mani, V., Zeng, Y., Ozen,  
904 M.O., Wang, L., et al., 2019. Loss of endothelium-derived Wnt5a is associated with reduced pericyte  
905 recruitment and small vessel loss in pulmonary arterial hypertension. *Circulation* 139, 1710–1724.

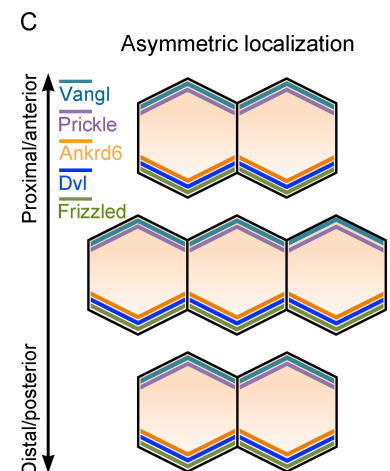
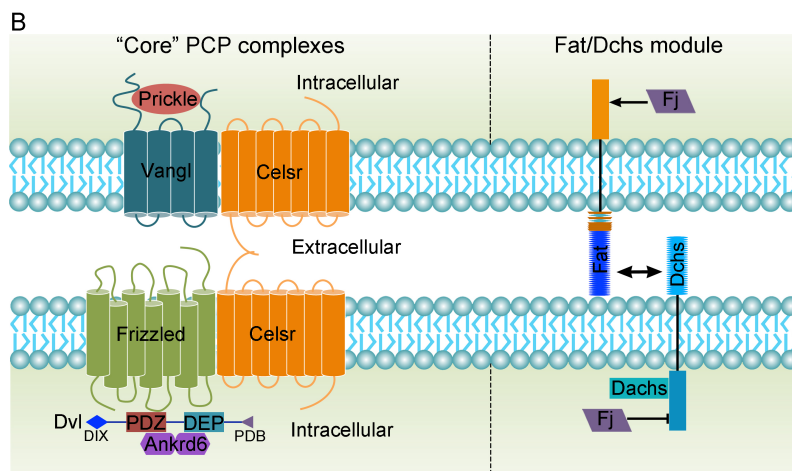
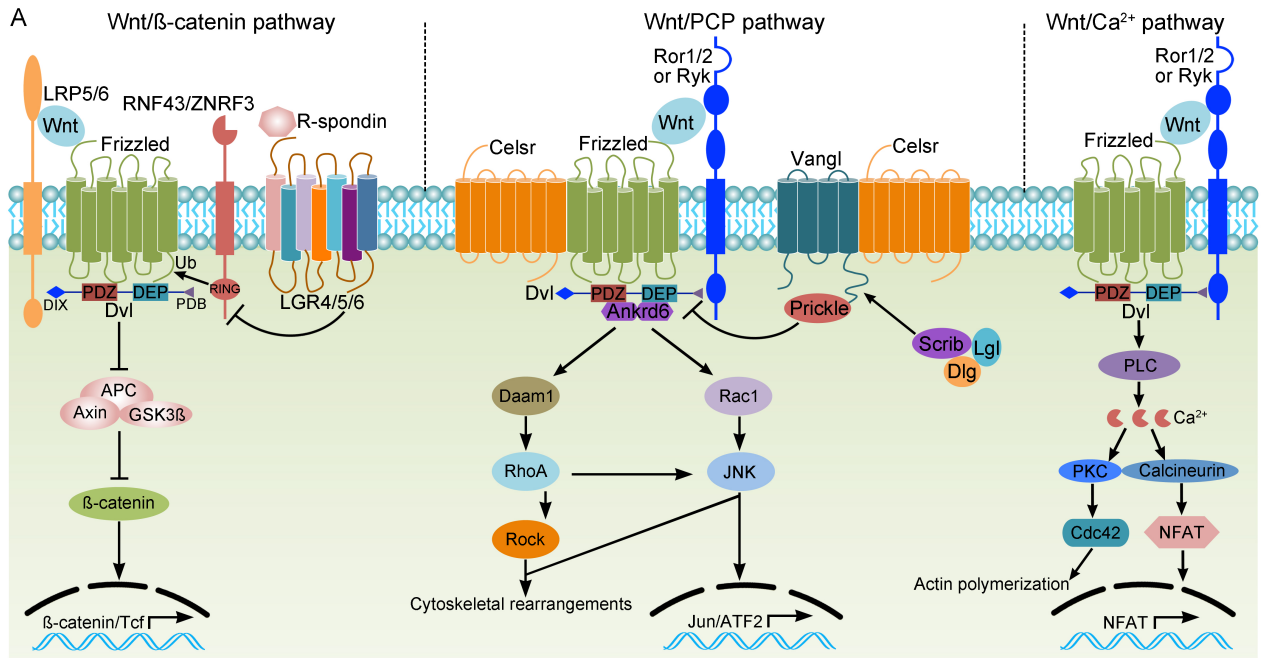
906 Yun, K., Ajima, R., Sharma, N., Costantini, F., Mackem, S., Lewandoski, M., Yamaguchi, T.P., Perantoni,  
907 A.O., 2014. Non-canonical Wnt5a/Ror2 signaling regulates kidney morphogenesis by controlling  
908 intermediate mesoderm extension. *Hum. Mol. Genet.* 23, 6807–6814.

909 Zhang, H., Bagherie-Lachidan, M., Badouel, C., Enderle, L., Peidis, P., Bremner, R., Kuure, S., Jain, S.,  
910 McNeill, H., 2019. FAT4 fine-tunes kidney development by regulating RET signaling. *Dev. Cell* 48, 780–  
911 792.e4.

912 Zhang, K., Yao, E., Lin, C., Chou, Y.T., Wong, J., Li, J., Wolters, P.J., Chuang, P.T., 2020. A mammalian  
913 Wnt5a-Ror2-Vangl2 axis controls the cytoskeleton and confers cellular properties required for  
914 alveologogenesis. *Elife* 9, e53688.

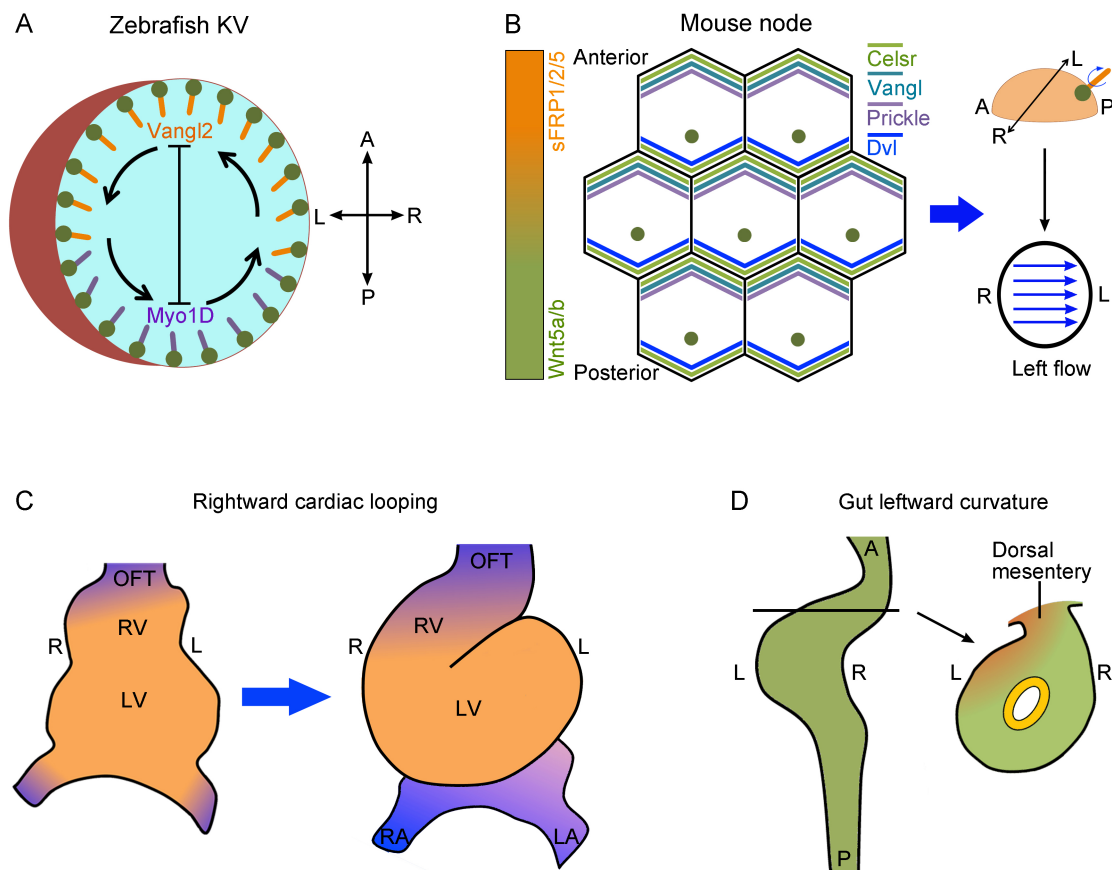
915 Zhou, W., Lin, L., Majumdar, A., Li, X., Zhang, X., Liu, W., Etheridge, L., Shi, Y., Martin, J., Van de Ven, W.,  
916 et al., 2007. Modulation of morphogenesis by noncanonical Wnt signaling requires ATF/CREB family-  
917 mediated transcriptional activation of TGFbeta2. *Nat. Genet.* 39, 1225–1234.

918



918  
 919 **Fig. 1.** Wnt signaling branches and asymmetric localization of PCP protein complexes. **A:** Wnt/β-  
 920 catenin signaling is activated by ligands binding to Fzd receptors and LRP5/6 (low density  
 921 lipoprotein receptor-related protein 5/6) co-receptors. The E3 RING ubiquitin ligases  
 922 RNF43/ZNRF3 mediate the ubiquitination (Ub) of Fzd receptors for lysosomal degradation. This  
 923 activity is inhibited by R-spondins binding to LGR4/5/6 (leucine-rich repeat containing G-protein  
 924 coupled receptors). The Wnt/PCP pathway is induced by interaction of Wnts with the Fzd/Ror1/2  
 925 (receptor tyrosine kinase-like orphan receptor 1/2) complex or the Fzd/Ryk (receptor tyrosine  
 926 kinase) complex. The activation of downstream effectors leads to cytoskeletal rearrangements  
 927 and/or transcription of ATF2 (activating transcription factor-2) target genes. The Scrib complex

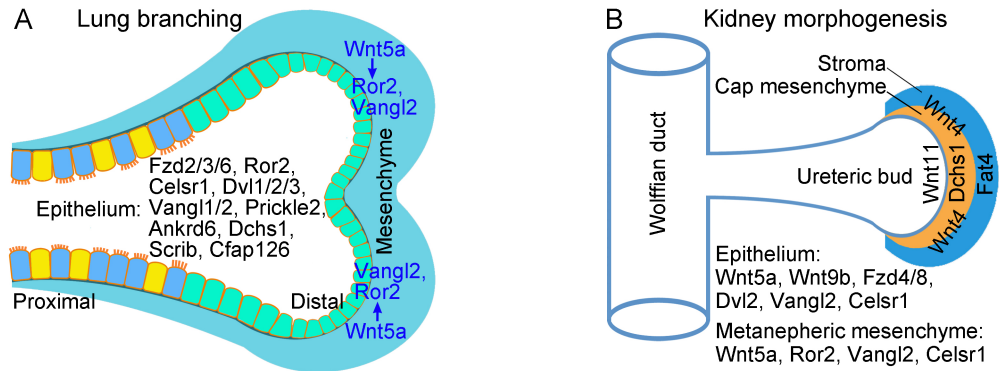
928 can function to regulate Vangl asymmetric localization. The Wnt/Ca<sup>2+</sup> branch triggers  
 929 phospholipase C (PLC) activity through heteromeric G proteins to induce calcium-dependent  
 930 responses. Dvl proteins mediate all Wnt signaling branches through distinct domains: N-terminal  
 931 DIX, central PDZ, C-terminal DEP, and extreme C-terminus PDZ domain-binding (PDB) motif. **B**:  
 932 The “core” PCP proteins function as two separately localized complexes, with Celsr forming  
 933 homodimers between neighboring cells. Fat and Dchs form heterodimers between adjacent cells,  
 934 acting as a ligand-receptor pair. Dachs is a Dchs-interacting unconventional myosin that functions  
 935 as a key effector of Fat/Dchs signaling. **C**: Asymmetric subcellular localization of “core” PCP  
 936 proteins along the proximal (anterior) and distal (posterior) axis in *Drosophila* epithelia.



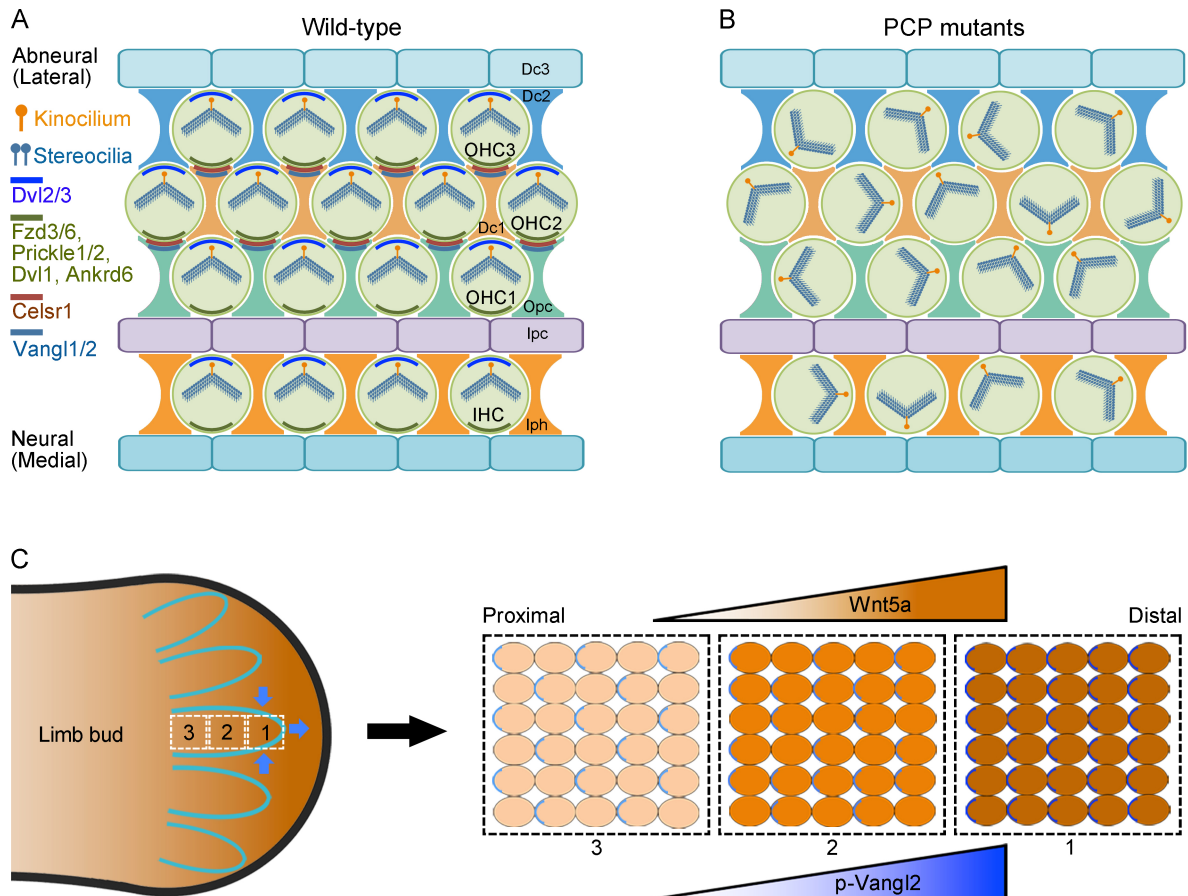
937  
 938 **Fig. 2.** Left-right organizers and asymmetric organogenesis. **A**: In the zebrafish KV, Vangl2 and  
 939 Myo1D coordinate leftward fluid flow (arrows) by regulating the localization of anteriorly (orange)  
 940 and posteriorly (purple) pointing cilia. **B**: In the mouse node, Wnt5a/b gradients along the AP axis  
 941 promote the asymmetric localization of PCP proteins. The posterior positioning of ciliary basal  
 942 bodies (green dots) at the dome-shaped apical surfaces of node cells and the posterior tilting of



943 cilia generate leftward fluid flow within the node. **C:** Asymmetric heart morphogenesis. Ventral  
 944 view shows rightward cardiac looping in E8.5-E9.5 mouse embryos. Progenitor cells derived from  
 945 the SHF (blue) promote heart tube elongation, contributing to the development of OFT, right  
 946 ventricule (RV) and the atria. RA, right atrium; LA, left atrium. **D:** Leftward curvature of gut tube.  
 947 Transverse section at the horizontal line shows Wnt/PCP-mediated mesenchymal condensation  
 948 (orange) on the left side of the dorsal mesentery in the chick embryo.



949  
 950  
 951 **Fig. 3.** PCP regulators in lung and kidney morphogenesis. **A:** At the earliest stage of lung  
 952 branching morphogenesis in E10.5 mouse embryos, mesenchyme-derived Wnt5a activates the  
 953 Ror2-Vangl2 cascade in the epithelium and mesenchyme to initiate distal lung morphogenesis.  
 954 PCP proteins display asymmetric localization in bronchial epithelium composed of multiciliated  
 955 cells and other cell types (yellow) as well as in distal lung epithelium. **B:** Schematic of ureteric  
 956 bud development in E11 mouse embryos shows the interaction between the Wolffian duct-  
 957 derived ureteric bud and its adjacent metanephric mesenchyme (stroma and cap mesenchyme).  
 958 PCP proteins act in the mesenchyme and/or in the ureteric bud to promote ureteric bud  
 959 branching, tubular elongation, and tubule diameter establishment. The Fat/Dchs polarity module  
 960 mediates stroma-to-cap mesenchyme signaling in nephrogenesis.



961

962 **Fig. 4.** Wnt/PCP signaling in stereociliary bundle orientation and proximal-distal limb elongation.

963 **A:** In the organ of Corti, hair cells are aligned with supporting cells, including inner phalangeal

964 cells (Iph), inner pillar cells (Ipc), outer pillar cells (Opc), and Deiter cells (Dc1, Dc2, and Dc3).

965 The arrowhead-shaped hair bundles are uniformly oriented toward the abneural (lateral) edge of

966 the sensory epithelium. **B:** PCP mutants display mis-orientations of hair bundles, but each hair

967 cell still retains polarized stereocilia. Severe PCP phenotypes lead to strongly shortened and

968 thickened cochlea with additional rows of IHCs or OHCs. **C:** The graded expression of Wnt5a in

969 the developing limb bud provides global cues to establish a gradient of Vangl2 phosphorylation

970 and localization (blue) along the proximal-distal axis. Vangl2 induces polarized mesenchymal cell

971 behaviors toward the overlying ectoderm (black line), ensuring limb elongation and chondrocyte

972 differentiation. Circles in dashed boxes depict limb chondrocyte condensates expressing Wnt5a

973 and phosphorylated Vangl2. Wnt5a also generates anisotropic active stresses and controls CE

974 movements (blue arrows) to promote the formation of digit-organizing centers for digit

975 specification and elongation.

**Table 1. Functions of PCP regulators in asymmetric organogenesis**

| Organs               | PCP proteins | Functions  | References  |
|----------------------|--------------|--|---|
| Left-right organizer | Wnt5a/b      | Asymmetric localization of “core” PCP proteins in node cells   | Minegishi et al., 2017  |
|                      | Dvl2/3       | Posterior positioning of ciliary basal bodies in node cells  | Hashimoto et al., 2010  |
|                      | Vangl1/2     | Posterior tilting of primary motile cilia in node cells; posterior orientation of anteriorly positioned cilia in the zebrafish KV (Vangl2) | Borovina et al., 2010; Antic et al., 2010; Song et al., 2010; Juan et al., 2018 |
|                      | Prickle1/2   | Asymmetric distribution of microtubules and actomyosin networks for posterior positioning of ciliary basal bodies in node cells            | Minegishi et al., 2017; Sai et al., 2022  |
|                      | Prickle3     | Basal body organization and cilia growth in <i>Xenopus</i> GRP   | Chu et al., 2016  |
|                      | Dchs1/2      | Vangl1 localization and basal body positioning in node cells   | Sai et al., 2022  |
|                      | JNK1/2       | Ciliogenesis and regulation of cilia length in the zebrafish KV  | Derrick et al., 2022  |
| Heart                | Wnt5a/b      | SHF deployment and AP elongation of the heart tube; OFT septation; polarization of actomyosin during heart tube remodeling (Wnt5b)         | Sinha et al., 2015; Merks et al., 2018; Li et al., 2019                         |
|                      | Wnt11        | OFT development and polarization of actomyosin networks during heart tube remodeling   | Zhou et al., 2007; Merks et al., 2018   |
|                      | Fzd4         | Microtubule stabilization and cellular polarization during arterial and arteriolar formation   | Descamps et al., 2012   |
|                      | Fzd2/7       | Redundantly involved in the closure of the ventricular septum  | Yu et al., 2012   |
|                      | Dvl1/2/3     | SHF deployment and OFT lengthening   | Sinha et al., 2012  |
|                      | Vangl2       | Polarized migration of myocardializing cells and OFT lengthening; formation of the coronary vasculature                                    | Phillips et al., 2005, 2008; Ramsbottom et al., 2014                            |

|      |               |  |  |
|------|---------------|--|--|
|      | Prickle1      | Polarized cell orientations and intercalations for OFT lengthening   | Gibbs et al., 2016   |
|      | Wdpcp         | Polarized migration of cardiomyocytes to invade the OFT cushion  | Cui et al., 2013   |
|      | Daam1/2       | Cytoskeletal organization and cell adhesion for protrusion of cardiomyocytes into OFT  | Li et al., 2011; Ajima et al., 2015  |
| Gut  | Wnt5a         | Leftward tilt and gut elongation; re-intercalation of post-mitotic cells into gut epithelium and post-mitotic filopodial pathfinding in nuclear trafficking; chemoattractant for oriented migration of mesenchymal cells during villus formation; homeostatic renewal of adult intestinal epithelium | Cervantes et al., 2009; Matsuyama et al., 2009; Welsh et al., 2013; Wang et al., 2018; Shoshkes-Carmel et al., 2018; Dush and Nascone-Yoder, 2019; Rao-Bhatia et al., 2020 |
|      | Ror2          | Midgut elongation (mesenchyme-derived Ror2 before phase I)   | Wang et al., 2020  |
|      | Ryk           | Midgut elongation by promoting post-mitotic filopodial pathfinding   | Wang et al., 2020  |
|      | Vangl2        | Oriented cell divisions to increase fore-stomach length; gut elongation and lumen formation; mesenchymal cell clustering in villus formation   | Matsuyama et al., 2009; Dush and Nascone-Yoder, 2019; Rao-Bhatia et al., 2020  |
|      | Daam2         | Mesenchymal condensation in the dorsal mesentery   | Welsh et al., 2013   |
|      | Fat4/Dchs1    | Mesenchymal cell clustering during villus formation  | Rao-Bhatia et al., 2020  |
|      | Cfap126       | Lineage priming and cell cycle exit at the base of the crypt for differentiation of Paneth and enteroendocrine cells   | Böttcher et al., 2021  |
| Lung | Wnt5a         | Distal lung morphogenesis and lung maturation; alveologenesi; mesenchymal cell polarization for trachea and esophagus formation  | Kishimoto et al., 2018; Li et al., 2020; Zhang et al., 2020  |
|      | Fzd2          | Epithelial cell shape changes to promote branch point formation  | Kadzic et al., 2014  |
|      | Fzd7          | Pulmonary endothelium-pericyte interactions during pulmonary angiogenesis  | Yuan et al., 2019  |
|      | Ror2          | Pulmonary vasculogenesis; alveologenesi  | Loscertales et al., 2008; Zhang et al., 2020   |
|      | Celsr1/Vangl2 | Maintenance of epithelial architecture; branching morphogenesis;   | Yates et al., 2010b; Li et al., 2020; Zhang et al.,  |

|        |                 |  |   |
|--------|-----------------|--|---|
|        | alveologenesis  | 2020   |   |
|        | Vangl1/Prickle2 | Airway epithelial homeostasis and adult lung function  | Vladar et al., 2016; Poobalasingam et al., 2017   |
|        | Scrib           | Tight junction integrity and epithelial cohesion in lumen morphogenesis  | Yates et al., 2013  |
|        | Cfap126         | Diameter formation in terminal lung bronchioles  | Gegg et al., 2014   |
|        | -----           |  |   |
|        | Wnt4            | Mesenchymal to epithelial transformation for epithelialization of the ureteric bud   | Stark et al., 1994; Kispert et al., 1998  |
|        | Wnt5a/Ror2      | Metanephric mesenchyme positioning for interaction with the Wolffian duct; epithelial tubular formation from the ureteric bud  | Nishita et al., 2014; Yun et al., 2014  |
|        | Wnt9b           | CE movements and polarized cell divisions for tubular diameter formation   | Karner et al., 2009   |
|        | Wnt11           | Attachment of nephron progenitors to the epithelial tip for nephrogenic niche integrity  | O'Brien et al., 2018  |
|        | Fzd4/8          | Growth, branching and proliferation of the ureteric epithelium   | Ye et al., 2011   |
|        | Dvl2            | Rosette-based CE movements during kidney tubule elongation   | Lienkamp et al., 2012   |
| Kidney | Vangl1/2        | Oriented cell divisions and CE movements in developing renal tubules; ureteric branching and glomerular maturation; organization of podocytes to protect glomerular injury in the adult (Vangl2) | Yates et al., 2010a; Rocque et al., 2015; Kunimoto et al., 2017                                   |
|        | Prickle1        | Cell arrangements in the collecting duct and renal tubules   | Liu et al., 2014  |
|        | Celsr1          | Rostrocaudal patterning of renal tubules and maturation of glomeruli; promoting ureteric tree growth at early stages and inhibiting tubule overgrowth at late stages                             | Brzóška et al., 2016  |
|        | Fat1/Scrib      | Cooperation with Fat4 in renal tubular elongation (Fat1); activation of Hippo signaling to regulate cell polarization and growth   | Saburi et al., 2012; Skouloudaki et al., 2009   |
|        | Fat4/Dchs1      | Oriented cell divisions for renal tubule elongation; Ureteric bud branching and tubule diameter formation; differentiation of ureteric epithelial  | Saburi et al., 2008; Das et al., 2013; Mao et al., 2015; Bagherie-Lachidan et al., 2015; Zhang et |

|            |  |   |
|------------|--|---|
|            | progenitors; polarization of cap mesenchyme; inhibition of ectopic ureteric bud formation and kidney duplication (Fat4)  | al., 2019   |
| Daam1      | Pronephric tubulogenesis; intercellular adhesion and epithelial tissue organization in CE and polarized movements  | Miller et al., 2011; Krneta-Stankic et al., 2021  |
| Fuz        | Cilia-dependent and -independent ureteric bud branching  | Wang et al., 2021   |
| <hr/>      |  |   |
| Wnts       | Cochlear extension and hair bundle orientation (interaction with Vangl2)   | Najarro et al., 2020  |
| Dvl1/2/3   | Cochlear extension and hair bundle orientation   | Montcouquiol et al., 2003; Wang et al., 2005  |
| Wnt11/Fzd7 | Alignment of support cells in zebrafish lateral line neuromasts  | Navajas Acedo et al., 2019  |
| Fzd1/2     | Hair bundle orientation (interaction with Vangl2)  | Yu et al., 2010   |
| Fz3/6      | Hair bundle orientation in the organ of Corti; cochlear innervation by type II spiral ganglion neurons   | Wang et al., 2006; Ghimire and Deans, 2019  |
| Vangl1/2   | Cochlear extension and hair bundle orientation; post-natal organization of supporting cells to promote the function of OHCs (Vangl2); axon turning toward the cochlear base to innervate OHCs (Vangl2) | Montcouquiol et al., 2003; Wang et al., 2005; Copley et al., 2013; Ghimire et al., 2018 |
| Inner ear  |  |   |
| Prickle1   | Neurite growth of type II spiral ganglion neurons toward OHCs  | Yang et al., 2017a  |
| Celsr1     | Earliest stages of hair cell polarity in the cochlea; hair bundle orientation in the vestibule associated with vestibular behaviors  | Curtin et al., 2003; Duncan et al., 2017  |
| Ankrd6     | Hair bundle orientation in the utricle; polarity and patterning of hair cells in the cochlea (interaction with Vangl2)   | Jones et al., 2014  |
| Fat1/4     | Cooperation in cochlear extension and patterning of OHCs   | Saburi et al., 2012   |
| PTK7       | Hair bundle orientation in OHC3; functioning in supporting cells to exert polarized contractile tension on hair cells  | Lu et al., 2004; Lee et al., 2012   |
| Scrib      | Planar polarization of stereociliary bundles (interaction with Vangl2)   | Montcouquiol et al., 2003, 2006   |

|          |          |   |   |
|----------|----------|---|---|
|          | Cfap126  | Kinocilium positioning and hair bundle morphogenesis in the cochlea   | Gegg et al., 2014   |
|          | Wdpcp    | Vangl2 asymmetric expression and kinocilium localization  | Cui et al., 2013  |
| -----    |          |   |   |
|          | Wnt5a    | Orientation of mesenchymal cell movements and divisions; chemoattractant for limb outgrowth; asymmetric localization and phosphorylation of Vangl2; generation of active stresses for the formation of digit-organizing centers | Yamaguchi et al., 1999; Gros et al., 2010; Wyngaarden et al., 2010; Gao et al., 2011; Parada et al., 2022 |
|          | Ror2     | Phalange development and elongation through the digit-organizing center; phosphorylation of Vangl2  | Witte et al., 2010; Gao et al., 2011  |
| Limb bud | Dvl1/2/3 | Interaction of casein kinase 1 with Vangl2 for Vangl2 phosphorylation   | Yang et al., 2017b  |
|          | Vang2    | Polarization of chondrocyte behaviors; elongation of proximal-distal axis; limb skeletal development  | Gao et al., 2011; Wang et al., 2011   |
|          | Prickle1 | Limb outgrowth; formation of distal skeletal elements; chondrocyte polarity and proximal-distal outgrowth of endochondral elements  | Yang et al., 2013; Liu et al., 2014   |
|          | Ryk      | Regulation of Vangl2 stability; interaction with Vangl2 in limb elongation  | Andre et al., 2012  |